inorganics

MDPI

Review

Iron–Sulfur Clusters toward Stresses: Implication for Understanding and Fighting Tuberculosis

Ingie Elchennawi and Sandrine Ollagnier de Choudens *

Laboratoire de Chimie et Biologie des Métaux, Université Grenoble Alpes, CNRS, CEA, F-38000 Grenoble, France
* Correspondence: sollagnier@cea.fr; Tel.: +33-4-3878-9122

Abstract: Tuberculosis (TB) remains the leading cause of death due to a single pathogen, accounting for 1.5 million deaths annually on the global level. *Mycobacterium tuberculosis*, the causative agent of TB, is persistently exposed to stresses such as reactive oxygen species (ROS), reactive nitrogen species (RNS), acidic conditions, starvation, and hypoxic conditions, all contributing toward inhibiting bacterial proliferation and survival. Iron–sulfur (Fe-S) clusters, which are among the most ancient protein prosthetic groups, are good targets for ROS and RNS, and are susceptible to Fe starvation. *Mtb* holds Fe-S containing proteins involved in essential biological process for *Mtb*. Fe-S cluster assembly is achieved via complex protein machineries. Many organisms contain several Fe-S assembly systems, while the SUF system is the only one in some pathogens such as *Mtb*. The essentiality of the SUF machinery and its functionality under the stress conditions encountered by *Mtb* underlines how it constitutes an attractive target for the development of novel anti-TB.

Keywords: tuberculosis; *Mycobacterium tuberculosis*; iron–sulfur cluster; SUF; ROS; RNS

Citation: Elchennawi, I.; Ollagnier de Choudens, S. Iron–Sulfur Clusters toward Stresses: Implication for Understanding and Fighting Tuberculosis. *Inorganics* **2022**, *10*, 174. https://doi.org/10.3390/inorganics10100174

Academic Editor: Ian Dance

Received: 26 August 2022
Accepted: 9 October 2022
Published: 18 October 2022

1. Introduction

Tuberculosis (TB) is the 13th leading cause of death worldwide. In 2020, it was anticipated that TB will rank as the second leading cause of death from a single infectious agent, after COVID-19 [1]. TB accounts for 1.5 million deaths annually on the global level. This situation is worsened by the alarming steady increase in the number of drug-resistant TB cases, with nearly half a million such cases in 2020 according to the WHO report (Global Tuberculosis report 2021).

Mycobacterium tuberculosis (*Mtb*), the causative agent of TB, has co-evolved with its human host to establish the continual loop of inhalation, infection, dormancy and transmission to other individuals. Throughout its life in the human host, the stresses to which *Mtb* is constantly exposed include reactive oxygen species (ROS), reactive nitrogen species (RNS), acidic conditions, starvation, and hypoxic conditions, all of which contribute to inhibiting the proliferation and survival of the bacterium. Indeed, during its pathogenic cycle, in the course of transmission from lungs to aerosols, *Mtb* experiences hypoxia and nutrient starvation. Once aerosols are inhaled inside the lungs, before encountering macrophages, *Mtb* is exposed to a hypophase containing short chain fatty-acids, surfactant proteins and glutathione. Upon phagocytosis by naïve macrophages, *Mtb* experiences increased levels of ROS. Inside activated macrophages, it experiences ROS, RNS and acidic pH. Finally, upon granuloma formation (organized aggregates of macrophages, often with characteristic morphological changes, and other immune cells), it experiences hypoxia, RNS and ROS [2]. Therefore, ROS and RNS are very often encountered by the pathogen *Mtb*.

Iron–sulfur (Fe-S) clusters, inorganic cofactors of proteins, are excellent targets for ROS and RNS and are susceptible to Fe starvation. *Mtb* was reported to contain at least 50 Fe-S containing proteins that harbor different structural types of Fe-S clusters participating mainly in energy production and conversion, transcription regulation and amino-acid transport and metabolism [3]. Fe-S cluster biogenesis in prokaryotes is achieved via complex

protein systems (ISC, SUF, NIF), which construct a nascent Fe-S cluster on a scaffold protein and then transfer the cluster to recipient proteins [4]. Many microorganisms contain several Fe-S assembly systems, while the SUF system is the only one in some pathogens, such as *Mtb* [5]. In order to better assess how to target *Mtb* and fight TB by interacting with the Fe-S metabolism (biogenesis and reactivity) of the pathogen, we report in this review (i) the stresses that target Fe-S cluster proteins within the host macrophages and granulomas; (ii) the putative Fe-S proteins/enzymes in *Mtb*, (iii) the way *Mtb* Fe-S cluster proteins are affected by these stresses, and (iv) how some *Mtb* Fe-S proteins sense and respond to such stresses to adapt to survive, including Fe-S biogenesis/repair. From this analysis, it is reasonable to believe that targeting Fe-S metabolism through the Fe-S biogenesis process could be a good strategy for TB control.

2. Stress Experienced by *Mtb*

During the course of infection, *Mtb* passes through a series of intracellular and extracellular locations, from alveolar macrophages to granulomas lesions, where *Mtb* is exposed to various types of stress. *Mtb* must therefore cope with a variety of host-mediated stresses, such as cell wall attacks, intra-phagosomal low pH, oxidative and nitrosative stress, hypoxia, iron limitation, nutrient starvation, and DNA damage [6,7].

2.1. Attacks on Mtb Cell Wall

The mycobacterial cell wall is considered as a key element in mediating resistance to host-related stresses as well as in intrinsic antibiotic resistance [8,9]. It is composed of a thick peptidoglycan layer, mycolic acid and arabinogalactan [9]. Hence, *Mtb* is subject to numerous attacks on its cell surface by host antimicrobial peptides present in the respiratory tract. Indeed, endogenous host defense peptides (HDPs) constitute the first-line defense against pathogens. Mammalian defensins (β-Defensin), granulysin, ubiquitin, and cathelicidins are cell-wall-targeting HDPs that exert an antimycobacterial activity by disturbing membrane permeability [10].

2.2. Harsh pH Conditions in Phagosomes

After phagocytosis by macrophages, *Mtb* remains in the phagosomes [11]. The host nuclear factor kappa B (NF-$_K$B) regulates the lysosomal hydrolytic enzymes, and acids release inside the phagosomes in order to destruct the pathogen's intracellular content (DNA, polysaccharides, lipids, proteins). NF-$_K$B also increases the production of membrane transport molecules responsible for the phagosome–lysosome fusion that could lead to pathogen elimination [12].

2.3. ROS and RNS

The host's interferon gamma (IFN-γ) and the tumour necrosis factor alpha (TNF-α) activate the functions of macrophages that generate reactive oxygen species (ROS) and reactive nitrogen species (RNS) in the mM range [11,13–15]. Reactive nitrogen species (sometimes referred as reactive nitrogen intermediates) include nitric oxide (•NO), peroxynitrite (ONOO-) and its reaction products, such as nitrogen dioxide ($\bullet NO_2$) and other types of chemically reactive free radicals (Figure 1). Peroxynitrite is formed from nitric oxide (produced via the enzymatic activity of inducible nitric oxide synthase (iNOS) expressed primarily in macrophages) and superoxide ($O_2^{\bullet -}$) (produced by NADPH phagocyte oxidase gp91^{phox} and gp47^{phox}) [16,17]. Molecular dioxygen is not the direct toxin of the reactive oxygen species (ROS). Because oxygen can easily take electrons, high oxygen concentrations favor the rapid formation of intracellular superoxide ($O_2^{\bullet -}$) and hydrogen peroxide (H_2O_2), which are poisons to cellular molecules. H_2O_2 is capable of giving rise, via "Fenton reaction"-type reactions, to the most deleterious radical species of oxidative stress, the hydroxyl radical OH$^\bullet$ (Figure 1) [18]. ROS and RNS damage DNA and proteins, in particular metalloproteins. Nitric oxide can readily react with transition metals relevant to biological processes including Fe, Cu and Mn; a well-known 'historical' ex-

ample includes the reaction of NO with hemoproteins such as hemoglobin [19], soluble guanylate cyclase [20] and cytochrome c oxidase [21]. NO or NO-derived reactive species also yield adducts with non-heme iron proteins such as Fe-S cluster proteins (see below). ROS damage some iron metalloenzymes such as mononuclear Fe(II) proteins, which are demetallated and subsequently mismetallated by alternative divalent metal ions [22], and also iron–sulfur cluster enzymes (see below). Although ROS and RNS damage numerous targets in a microbial cell, including metal centers, thiols, protein tyrosines, nucleotide bases and lipids, Fe-S clusters are exceptionally susceptible cellular cofactors [23,24].

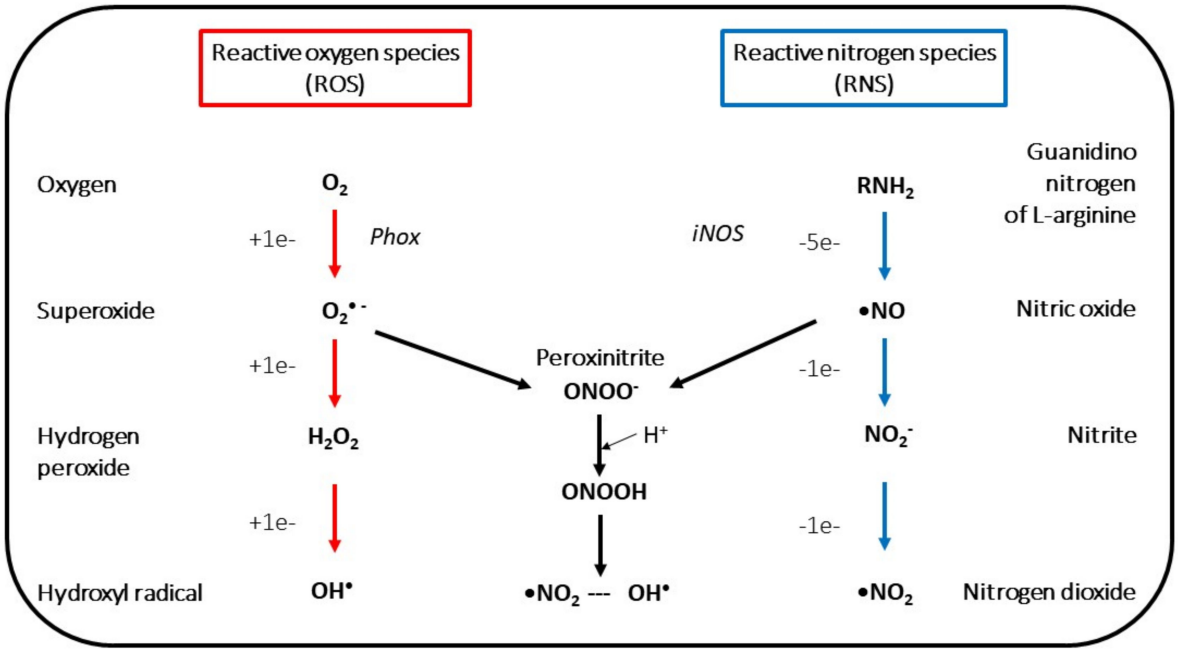

Figure 1. Reactive oxygen and nitrogen species production in mammalian cells.

2.4. Starvation

Human necrotic granulomas are a pathologic hallmark and one of the main features of the host's immune response to *Mtb* [25]. The environment inside granulomas is poor in nutrients such as leucine, arginine, tryptophan and phosphate [26–29]. Another major host immune response to *Mtb* infection is iron starvation. Iron is an essential element for *Mtb* as it has a crucial structural and catalytic role in transcription factors and enzymes [30]. Fe is vital for the survival and persistence of *Mtb* [31]. The host lowers serum iron levels by overproducing iron-binding molecules such as lactoferrin, transferrin, and ferritin, as well as initiating iron withdrawal from the circulation by macrophages [32]. Therefore, there is restricted iron availability within the host.

2.5. Hypoxia

Mtb is an obligate aerobe microorganism that preferentially replicates and resides in the most oxygen-rich regions in the human body [33], in agreement with its presence within patients' open airways. The granuloma environment is known for its harsh conditions and limited oxygen, making the microenvironment no longer permissive for bacterial persistence and replication. Under hypoxic conditions, the expression of up to 100 genes involved in DNA synthesis, protein synthesis, and cellular division is altered [34].

Despite these impressive stresses, *Mtb* has the ability to adopt strategies to counteract these detrimental conditions to persist in the host [6]. We will discuss *Mtb* responses to ROS, RNS, and Fe limitation, which directly and adversely impact a family of metalloproteins that we focus on in this review, namely the iron–sulfur proteins (see below).

3. Fe-S Clusters Proteins in *Mtb*

The first protein with an Fe-S cluster was discovered in the early 1960s, due to the presence of an EPR signal at g = 1.9 in the NADH dehydrogenase that had never been observed before [35]. Iron and inorganic sulfur determinations, as well as structure determinations, revealed a completely new chemical composition. Since then, the number of identified proteins containing an Fe-S center has been increasing due to the combination of spectroscopic, biochemical, crystallographic and chemical studies (synthesis of structural analogues of active sites) [36–41]. Fe-S clusters are inorganic prosthetic groups composed exclusively of iron and inorganic sulfides contained in proteins [42]. In general, Fe-S clusters are coordinated by thiolate from cysteine residues of the proteins and are involved in the redox reaction, and in particular in electron transport. The most common are Fe_2S_2 and Fe_4S_4 clusters, although more complex architectures are known [43]. The chemical and structural versatility of Fe-S clusters is uniquely achieved by combining the individual chemical properties of Fe and S, which has enabled Fe-S proteins to undertake many important, sometimes essential, functions other than electron transport, such as substrate activation, environmental sensors, gene regulation and structural elements [43–45]. A bioinformatic analysis has revealed that *Mtb* contains at least 50 Fe-S proteins [3] which is half of the known Fe-S proteins in *E. coli* [46] (*Mtb* and *E. coli* have comparable genome sizes). The majority of these proteins coordinate a Fe_4S_4 cluster, but some other types of Fe-S exist, such as FeS_4 (rubredoxin), Fe_2S_2, and Fe_3S_4 clusters. A detailed analysis of these putative Fe-S proteins (their sequence and function), completed by an analysis of the literature on known Fe-S proteins in *Mtb*, and by a thorough study of characterized bacterial Fe-S proteins whose genes exist in *Mtb*, made it possible to draw up a list of 58 Fe-S proteins (Table 1). Predicted functions were associated with these putative *Mtb* Fe-S proteins. Among these are intermediary metabolism and respiration, transcriptional regulation (WhiB proteins), cell wall and cell process, information pathway, virulence (Table 1), showing that *Mtb* exploits Fe-S clusters containing proteins for respiration, metabolism, DNA repair, antibiotic resistance and persistence. Obviously, Fe-S proteins appear to be critical to *Mtb*'s life. Then, based on data available in the literature (systematic genome-wide studies in RvH37 *Mtb* strain, including studies using Tn-seq in rich and minimal media) [47–51], we report essential *Mtb* Fe-S proteins in vitro (essential = indispensable for growth and/or survival) (Table 1, column 5) [47–51]. A set of 20 Fe-S proteins, out of the total 58, are predicted to be essential (Table 1, column 5). Recently, genome-wide gene expression tuning has revealed diverse vulnerabilities of *Mtb*. A CRISPR interference system, using *Mtb* as a model organism, has been used to titrate gene expression and uncover gene vulnerability, redefining the concept of essential genes and identifying antimicrobial targets [52]. The vulnerability of a gene was defined by its vulnerability index (VI). In simple terms, the analysis of the gene expression tuning enables a VI value to be obtained; if negative, this means that the gene is essential (Essentiality: Yes). On the contrary, a positive value of the VI (or a low negative value of the VI) indicates that the gene is not essential (Essentiality: No) (Table 1, column 6). Combining all these data (columns 5 and 6), among the 58 predicted *Mtb* Fe-S proteins, 16 are predicted as essential, both highlighted using the CRISPR interference system and the Himar1 transposon mutagenesis. Rv1465, Rv3109, Rv2391 and Rv2392, which have been predicted to be essential from in vitro growth using Tn-seq, are predicted not to be essential from the CRISPR system with a vulnerability index (VI) of −1.142, 1.107, 0.514 and −0.34, respectively [52]. Therefore, they are not considered as essential.

Table 1. Predicted Fe-S proteins in *Mtb* and their essentiality. Genome-wide gene expression tuning using CRISPR interference system. Vulnerability index (VI) and gene essentiality (yes/no) are given (data extracted from DataS2 in [52]). For comparison, genes encoding the targets of first-line TB therapy (*rpoB*, *inhA*, and *embAB*) have a VI value of −9.5, −9.9, −5.85 and −6.45, respectively [52]. Gene for in vitro growth of H37Rv by analysis of saturated Himar1 transposon libraries [47]. Gene for in vitro growth of H37Rv in a *Mtb*YM rich and *Mtb* minimal media by Tn-seq studies [50]. Gene by Himar1 transposon mutagenesis in H37Rv and CDC1551 strains [48,49,51]. Essentiality is defined as a gene essential for growth and/or survival. Even though NuoI (Rv3153) displays a vulnerability index value (VI: −2.127) in the range of a potential vulnerable gene, the high variability between the lower and higher bounds of the vulnerability index makes this gene likely non-vulnerable.

Gene Name	Functional Category	Name	Predicted Fe-S	Essentiality	VI/ Essentiality [52]
Rv0247c	Intermediary metabolism and respiration	Succinate dehydrogenase	Fe_4S_4	No [47,48,50]	1.083/No
Rv0252	Intermediary metabolism and respiration	Nitrite reductase NAD(P)H large subunit [FAD flavoprotein] NirB	Fe_2S_2	No [47,49,50]	1.106/No
Rv0338c	Intermediary metabolism and respiration	Heterodisulfide reductase IspQ	Fe_2S_2 + Fe_4S_4	No [50], Yes [47–49]	−5.232/Yes
Rv1162	Intermediary metabolism and respiration	Respiratory nitrate reductase NarH	Fe_4S_4	No [47–51]	1.259/No
Rv1161	Intermediary metabolism and respiration	Respiratory nitrate reductase NarG	Fe_4S_4	No [47,49,50]	1.345/No
Rv1177	Intermediary metabolism and respiration	Ferredoxin FdxC	Fe_4S_4 Fe_3S_4	Yes [47–50]	-4.792/Yes
Rv1465	Intermediary metabolism and respiration	Nitrogen-fixation-related protein	Fe_2S_2	Yes [47–50]	−1.14/No
Rv1475c	Intermediary metabolism and respiration	Aconitase Acn	Fe_4S_4	Yes [47–50]	−2.18/Yes
Rv1553	Intermediary metabolism and respiration	Fumarate reductase FrdB	Fe_4S_4	No [47–51]	−1.393/No
Rv2195	Intermediary metabolism and respiration	Rieske protein QcrA	Fe_2S_2	Yes [47–50]	−8.875/Yes
Rv2776c	Intermediary metabolism and respiration	Oxidoreductase	Fe_2S_2	No [47–50]	0.734/No
Rv3230c	Intermediary metabolism and respiration	Oxidoreductase	Fe_2S_2	No [47,49,50] Yes [48]	0.848/No
Rv3151	Intermediary metabolism and respiration	NADH dehydrogenase I NuoG	Fe_4S_4	No [47,50]	0.727/No

Table 1. *Cont.*

Gene Name	Functional Category	Name	Predicted Fe-S	Essentiality	VI/ Essentiality [52]
Rv3153	Intermediary metabolism and respiration	NADH dehydrogenase I NuoI	Fe_4S_4	No [47,49,50]	−2.127/No
Rv3250c	Intermediary metabolism and respiration	Rubredoxin RubB	FeS_4	No [47–49]	0.681/No
Rv3251c	Intermediary metabolism and respiration	Rubredoxin RubA	FeS_4	No [47–51]	0.22/No
Rv3316	Intermediary metabolism and respiration	Succinate dehydrogenase SdhC	Fe_4S_4	No [47–50]	0.688/No
Rv3318	Intermediary metabolism and respiration	Succinate dehydrogenase SdhA	Fe_4S_4	No [47,49–51]	1.32/No
Rv3436c	Intermediary metabolism and respiration	Glucosamine-fructose-6-phosphate aminotransferase GlmS	Fe_4S_4	Yes [47–50]	−8.478/Yes
Rv3319	Intermediary metabolism and respiration	Succinate dehydrogenase SdhB	Fe_4S_4	No [47–50]	1.147/No
Rv3554	Intermediary metabolism and respiration	FdxB	Fe_2S_2	No [47–51]	1.141/No
Rv2007c	Intermediary metabolism and respiration	FdxA	Fe_4S_4 and Fe_3S_4	No [47,48,50]	0.494/No
Rv3674c	Information pathway	Endonuclease III Nth	Fe_4S_4	No [47–51]	0.789/No
Rv1259	Information pathway	Adenine DNA glycosylase	Fe_4S_4	No [47–50]	1.236/No
Rv3571	Intermediary metabolism and respiration	Reductase component of 3-ketosteroid-9-alpha-hydroxylase KshB	Fe_2S_2	No [47–51]	1.112/No
Rv1485	Intermediary metabolism and respiration	Ferrochelatase (HemZ)	Fe_2S_2	Yes [47–50]	−3.427/Yes
Rv1594	Intermediary metabolism and respiration	Quinolinate synthase (NadA)	Fe_4S_4	Yes [47–50]	−8.86/Yes
Rv1937	Intermediary metabolism and respiration	Oxygenase	Fe_2S_2	No [47,49–51]	0.808/No
Rv0022c	Regulatory protein	Transcriptional regulatory protein WhiB5	Fe_4S_4	No [47–50]	0.687/No
Rv1287	Regulatory protein	Conserved hypothetical protein Rrf family	Fe_4S_4 or Fe_2S_2	No [47–50]	−0.197/No

Table 1. *Cont.*

Gene Name	Functional Category	Name	Predicted Fe-S	Essentiality	VI/ Essentiality [52]
Rv3197a	Regulatory protein	Transcriptional regulatory protein WhiB-like WhiB7	Fe_4S_4	No [47,48,50]	−0.17/No
Rv3219	Regulatory protein	Transcriptional regulatory protein WhiB-like WhiB1	Fe_4S_4	Yes [47,50] No [49]	−10.916/Yes
Rv3260c	Regulatory protein	Transcriptional regulatory protein WhiB2	Fe_4S_4	Yes [47,50]	−7.373/Yes
Rv3416	Regulatory protein	Transcriptional regulatory protein WhiB3	Fe_4S_4	No [47–50]	−0.205/No
Rv3681	Regulatory protein	Transcriptional regulatory protein WhiB4	Fe_4S_4	No [47–50]	0.69/No
Rv3862c	Regulatory protein	Transcriptional regulatory protein WhiB6	Fe_4S_4	No [47–51]	0.309/No
Rv0189c	Intermediary metabolism and respiration	Dihydroxy-acid dehydratase IlvD	Fe_2S_2	Yes [47–49] No [50]	−7.985/Yes
Rv0492c	Intermediary metabolism and respiration	Oxidoreductase GMC-type	Fe_4S_4	No [47–50]	0.821/No
Rv0886	Intermediary metabolism and respiration	NADPH adrenodoxin oxidoreductase FprB	Fe_4S_4	No [47,49–51]	0.962/No
Rv2391	Intermediary metabolism and respiration	Sulfite reductase SirA	Fe_4S_4	No [47] Yes [49,50]	0.514/No
Rv2392	Intermediary metabolism and respiration	Adenosine 5′-phosphosulfate reductase (CysH)	Fe_4S_4	Yes [47–50]	−0.34/No
Rv2988c	Intermediary metabolism and respiration	3-isopropylmalate dehydratase (LeuC)	Fe_4S_4	Yes [48]; No [47,50]	−2.19/No
Rv0808	Intermediary metabolism and respiration	Amido-phosphoribosyl transferase PurF	Fe_4S_4	Yes [47–49] No [50]	−7.635/Yes
Rv1616	Cell wall and cell process	Rubredoxin	FeS_4	No [47,49,50]	0.517/No
Rv0863	Conserved hypothetical	Unknown	Fe_4S_4	No [47–50]	0.183/No
Rv3242c	Virulence, detoxification, adaptation	Phosphoribosyl transferase	Fe_4S_4	No [47–51]	0.984/No
Rv3161c	Intermediary metabolism and respiration	Dioxygenase	Fe_2S_2	No [47–50]	0.714/No
Rv3858c	Intermediary metabolism and respiration	Glutamate synthase GltD	Fe_4S_4	Yes [47–49]	−9.128/Yes

Table 1. *Cont.*

Gene Name	Functional Category	Name	Predicted Fe-S	Essentiality	VI/ Essentiality [52]
Rv3859c	Intermediary metabolism and respiration	Glutamate synthase GltB	Fe_4S_4	Yes [47–49]	−11.539/Yes
Rv0322	Intermediary metabolism and respiration	UDP-glucose 6-dehydrogenase UdgA	Fe_3S_4	No [47–50]	0.898/No
Rv0423c	Intermediary metabolism and respiration	Phosphomethyl Pyrimidine synthase ThiC	Fe_4S_4	Yes [47–49]	−5.557/Yes
Rv3109	Intermediary metabolism and respiration	Molybdenum cofactor biosynthesis MoaA	Fe_4S_4	No [47,50] Yes [48,49]	1.107/No
Rv1173	Intermediary metabolism and respiration	F420 biosynthesis FbiC	Fe_4S_4	No [47,50] Yes [48]	0.962/No
Rv2733c	Translation, ribosomal structure and biogenesis	tRNA 2-methylthio-N(6)-dimethylallyl-adenosine synthase MiaB	Fe_4S_4	No [47–50]	−1.184/No
Rv1589	Intermediary metabolism and respiration	Biotin synthase BioB	Fe_4S_4 and Fe_2S_2	No [47,49–51] Yes [48]	−0.169/No
Rv2218	Intermediary metabolism and respiration	Lipoate Synthase LipA	2x Fe_4S_4	Yes [47–50]	−5.037/Yes
Rv1110	Cell wall and cell process	LytB2/IspH	Fe_4S_4	Yes [47,48,50]	−9.422/Yes
Rv2204c	Conserved hypothetical	Fe-S insertion protein	Fe_2S_2	No [47,49]	−1.674/No

Among the essential Fe-S proteins, both highlighted by in vitro growth using Tn-seq studies and CRISPR technique, are aconitase Acn (Rv1475c), ferredoxin FdxC (Rv1177), quinolinate synthase NadA (Rv1594), glucosamine-fructose 6-phosphate aminotransferase GlmS (Rv3436c), WhiB1 (Rv3219) and WhiB2 (Rv3260c), IlvD (Rv0189), QcrA (Rv2195), ferrochelatase HemZ (Rv1485), amido-phosphoribosyl transferase PurF (Rv0808), 4-hydroxy-3-methylbut-2-enyl diphosphate reductase 2 (Rv1110), Lipoate synthase (Rv2218), Phosphomethylpyrimidine synthase (Rv0423c), heterodisulfide reductase (Rv0338c), and glutamate synthases (Rv3858c and Rv3859c) (Table 1). Although these proteins/enzymes represent interesting therapeutic targets, few have been characterized at a molecular level as Fe-S proteins.

Mtb Aconitase (AcnA) functions as a tricarboxylic acid (TCA) cycle enzyme converting isocitrate to cis-aconitate, likely using its Fe-S cluster as a catalyst. Upon iron depletion (apo form), it behaves like an iron-responsive protein (IRP), binding to the selected iron-responsive elements (IREs) in vitro. Indeed, the apo form of AcnA (no Fe-S cluster) functions as an RNA-binding regulatory protein that binds to selected IRE-like sequences, present within the UTRs (untranslated regions) of 3′ thioredoxin (trxC) and 5′ iron-dependent repressor and activator (IdeR) mRNA [53]. These two activities of *Mtb* Acn are mutually exclusive, pointing to its role in iron homeostasis.

Mtb IlvD is a dihydroxy-acid dehydratase, a key enzyme involved in branched-chain amino acid (BCAA) biosynthesis, which catalyzes the synthesis of 2-ketoacids from dihydroxyacids [54]. Recently, the IlvD crystal structure was solved at 1.88 Å resolution,

revealing an Fe_2S_2 cluster coordinated by three cysteine residues and one exchangeable water molecule or hydroxide [55]. Spectroscopic studies suggested that the substrate binds to the cluster, strongly suggesting that it acts as a Lewis acid similarly to *E. coli* IlvD [56]. IlvD (Rv0189c) has no mammalian counterpart and therefore constitutes a very interesting therapeutic target against TB. *Mtb*-IlvD is inhibited by a herbicide, aspterric acid, that might be a potential lead compound for the design of novel anti-TB drugs [55].

Ferredoxin (FdxC) is a protein that transfers electrons, being possibly involved in a wide variety of metabolic reactions. From its amino-acid sequence, it could bind both Fe_3S_4 and Fe_4S_4 clusters, even though this has to be demonstrated in *Mtb*.

D-fructose 6-phosphate aminotransferase (GlmS) is involved in the carbohydrate derivative biosynthetic process, catalyzing the first step in hexosamine metabolism and converting fructose-6P into glucosamine-6P using glutamine as a nitrogen source [57]. *Mtb* GlmS has not yet been characterized in vitro like GlmS enzymes from other microorganisms.

Ferrochelatase HemZ is involved in coproporphyrin-dependent heme b biosynthesis [58]. It catalyzes the insertion of ferrous iron into protoporphyrin IX to form protoheme, which serves as a prosthetic group in a wide array of metabolic pathways; well-known enzymes include respiratory cytochromes, hemoglobin, cytochrome P450s, catalases, and other hemoproteins. *Mtb* ferrochelatase does not use protoporphyrin as an intermediate but, instead, inserts ferrous iron into coproporphyrin, resulting in the formation of coproheme [58]. This enzyme incorporates a Fe_2S_2 cluster ligated by four cysteine residues, and the cluster is essential for the stability and function of the protein, even though its role is not yet known [59].

QcrA is an iron–sulfur subunit of the cytochrome bc1 complex, an essential component of the respiratory electron transport chain required for ATP synthesis [60]. The bc1 complex catalyzes the oxidation of menaquinol and the reduction of cytochrome c in the respiratory chain. The bc1 complex operates through a Q-cycle mechanism that couples electron transfer to generation of the proton gradient that drives ATP synthesis. *Mtb* QcrA was identified as a high-confidence drug target [61] and proposed to contain an Fe_2S_2 cluster, even though this has yet to be demonstrated.

Amidophosphoribosyl transferase, PurF, is involved in purine metabolism, catalyzing the formation of phosphoribosylamine from phosphoribosylpyrophosphate (PRPP) and glutamine [62]. Even though it was not characterized at a molecular level, *Mtb* PurF is proposed to bind a Fe_4S_4 cluster like other bacterial amido-phosphoribosyl transferases [63].

Mtb synthesises the isoprenoid precursor, isopentenyl diphosphate (IPP), via the non-mevalonate or 1-deoxy-D-xylulose 5-phosphate (MEP/DOXP) pathway, in contrast to the human mevalonate pathway [64,65]. LytB (IspH) (Rv1110) is a 4-hydroxy-3-methylbut-2-enyl diphosphate reductase involved in the terminal step of the MEP/DOXP pathway catalyzing the conversion of (E)-4-hydroxy-3-methyl-but-2-enyl pyrophosphate (HMB-PP) into IPP and dimethylallyl pyrophosphate (DMAPP). The LytB structure has been determined in several species and the enzyme contains an iron–sulfur Fe_4S_4 cluster [66–68]. *Mtb* has two homologs of lytB (Rv3382c and Rv1110). Only LytB2 is essential in *Mtb*, confirming that LytB1 is not able functionally to complement the loss of lytB2 [69]. *Mtb* LytB2 contains cysteine residues that bind Fe-S clusters in *E. coli* LytB [70], strongly suggesting that LytB2 is an Fe-S enzyme.

Lipoic acid is a simple cofactor consisting of an eight-carbon fatty acyl chain containing sulfur atoms at C6 and C8. It is synthesized de novo in a two-step process. The first step, catalyzed by octanoyl transferase (LipB), is the transfer of an n-octanoyl chain from octanoyl-acyl carrier protein (ACP) to a lypoyl carrier protein [71,72]. The second enzyme, LipA, catalyzes the stepwise insertion of sulfur at C6 and C8 of the octanoyl chain, yielding the final cofactor. Mechanistic studies have focused on LipA from *E. coli*. LipA is a member of the radical SAM superfamily of enzymes, which use a $[4Fe{-}4S]^{+}$ cluster to catalyze the reductive cleavage of S-adenosyl-L-methionine (SAM) to methionine, and a reactive 5′-deoxyadenosyl 5′-radical (5′dA•). The role of the 5′-dA• is to initiate radical catalysis by abstracting target hydrogen atoms (H•), from unactivated or poorly

activated carbon centers. LipA harbors two Fe_4S_4 clusters essential for activity [73]. One cluster is coordinated by the three cysteines of the canonical CX3CX2C motif and the SAM coordinates the fourth iron site; this is the cluster where the radical chemistry occurs (RS cluster). The second cluster is ligated by cysteines of the CX4CX5C motif and a serine residue, and it acts as a sulfur donor for lipoic acid formation [74,75]. Lipoyl synthase from *Mtb* (Rv2218) contains two Fe_4S_4 clusters and converts an octanoyl peptide substrate to the corresponding lipoyl peptide product via the same C6-monothiolated intermediate as that observed in the *E. coli* LipA reaction [76]. Moreover, LipA from *Mtb* can complement a lipA mutant of *E. coli*, demonstrating the commonalities of the two enzymes [76].

The thyamine pyrimidine synthase (Rv0423c) catalyzes the complex rearrangement of aminoimidazole ribonucleotide (AIR) to 4-amino-5-hydroxymethyl-2-methylpyrimidine phosphate (HMP-P) in the thiamin biosynthetic pathways of bacteria and plants [77] and is an example of a non-canonical radical SAM enzyme with the CX2CX4C motif coordinating the Fe-S cluster [78]. ThiC contains only one Fe_4S_4 cluster that is essential for its activity [79]. Structures of ThiC with Fe_4S_4 clusters were solved [80], leaving no doubt that ThiC is an Fe-S enzyme. Structural and functional characterization of *Mtb* ThiC remains to be carried out.

IspQ (iron–sulfur protein Q) (Rv0338c) was proposed (from Tuberculist) to encode a putative iron–sulfur heterodisulfide reducatase. This is a membrane-bound redox enzyme recently reported to be involved in energy metabolism or redox sensing [81]. This enzyme is the primary target of two 6,11-Dioxobenzo[f]pyrido[1,2-a]indoles (DBPI), molecules that kill *Mtb* [81]. Even though this protein is suggested to bind two Fe-S clusters (based on heterodisulfide reductase from *Methanococcus thermolithotrophicus*) [81], this has to be demonstrated through biochemical and structural approaches.

Glutamate synthases carry out the synthesis of two molecules of L-glutamate from L-glutamine and 2-oxoglutarate (2-OG) by catalyzing the reductive transfer of the glutamine amide group to the C(2) carbon of 2-OG. On the basis of the primary structures of glutamate synthases from different sources and the known biochemical properties, three distinct classes of enzymes can be distinguished [82]: (class I) Ferredoxin-dependent glutamate synthase is an iron–sulfur (a Fe_3S_4) and FMN-containing enzyme that has been detected in chloroplasts of higher plants, cyanobacteria and algae; (class II) NADPH-dependent glutamate synthase is mostly found in bacteria; the enzyme is composed of two tightly bound dissimilar subunits, which form the αβ holoenzyme containing one flavin adenine dinucleotide (FAD) and one FMN cofactor, and three distinct iron–sulfur clusters, one Fe_3S_4 center and two Fe_4S_4 clusters; and (class III) NADH-dependent glutamate synthase is poorly characterized and is mainly found in fungi, lower animals, seeds and roots of plants [83]. In all glutamate synthases studied so far, Fe-S clusters serve to transfer electrons. *Mtb* glutamate synthase, both small and large subunits (GltB and GltD, respectively) were expressed in *E. coli* and purified, unfortunately without its Fe-S clusters [84].

Quinolinate synthase (NadA) catalyzes a unique condensation reaction between iminoaspartate and dihydroxyacetone phosphate, affording quinolinic acid, a central intermediate in the biosynthesis of nicotinamide adenine dinucleotide (NAD). NadA from *Mtb* contains a Fe_4S_4 cluster coordinated by three conserved cysteine residues, the fourth catalytic iron site being coordinated by a water molecule [85–87]. Implicated in the biosynthesis of an essential cofactor, NadA has been suggested to be a noteworthy target for the design of antibacterial agents against *Mtb*, like the other genes involved in NAD biosynthesis and recycling. The catalytic mechanism has been well studied using biochemical and structural approaches [88–90] allowing the design of NadA inhibitors [91,92]. Unfortunately, these inhibitors have not been proven to be active *in cellulo* on *Mtb* NadA.

The WhiB transcriptional regulators (WhiB1-WhiB7). WhiB proteins are members of the WhiB-like (Wbl) family, which contain proteins characterized by a small size (80–140 residues) and the presence of four invariant conserved cysteine residues (Cys(x)nCys(x2) Cys(x5)Cys) involved in the binding of a Fe_4S_4 cluster essential for their function. They share another conserved sequence of five residues (G [V/I]WGG), located at one end of a loop that follows the last conserved cysteine. Structural predictions suggest this loop to be

a key element for interacting with cellular molecules [93]. The *Mtb* genome encodes seven paralogues of Wbl family proteins, WhiB1 (Rv3219), WhiB2 (Rv3260c), WhiB3 (Rv3416), WhiB4 (Rv3681c), WhiB5(Rv0022c), WhiB6 (Rv3862c), and WhiB7 (Rv3197A). All WhiB proteins are transcriptional regulators and, except for WhiB2, they all have been described to display a disulfide reductase activity (Figure 2) [94]. All *Mtb* WhiB proteins are important for *Mtb* survival within the host, even though only WhiB1 and WhiB2 are essential proteins. *Mtb* WhiB proteins are able to detect stress signals (through their Fe-S cluster), allowing *Mtb* to adjust its metabolism to survive under stress conditions in macrophages and to enter dormancy [3]. In the whole, *Mtb* WhiB proteins are involved in regulation of virulence (WhiB1, WhiB3, WhiB4, WhiB6), antibiotic resistance (WhiB7), and the regulation of cell division (WhiB2) [93,95]. *Mtb* WhiB proteins have low sequence homology but all contain an O_2- and NO-sensitive Fe_4S_4 cluster, raising the question as to how they can support distinct cellular function within *Mtb*. Recent studies shed light on the biochemical function of WhiB as transcriptional factors and sensors of NO and O_2, and suggest that WhiB evolution has created diversity in protein–protein interactions, Fe-S sensitivity and ability to bind DNA [93].

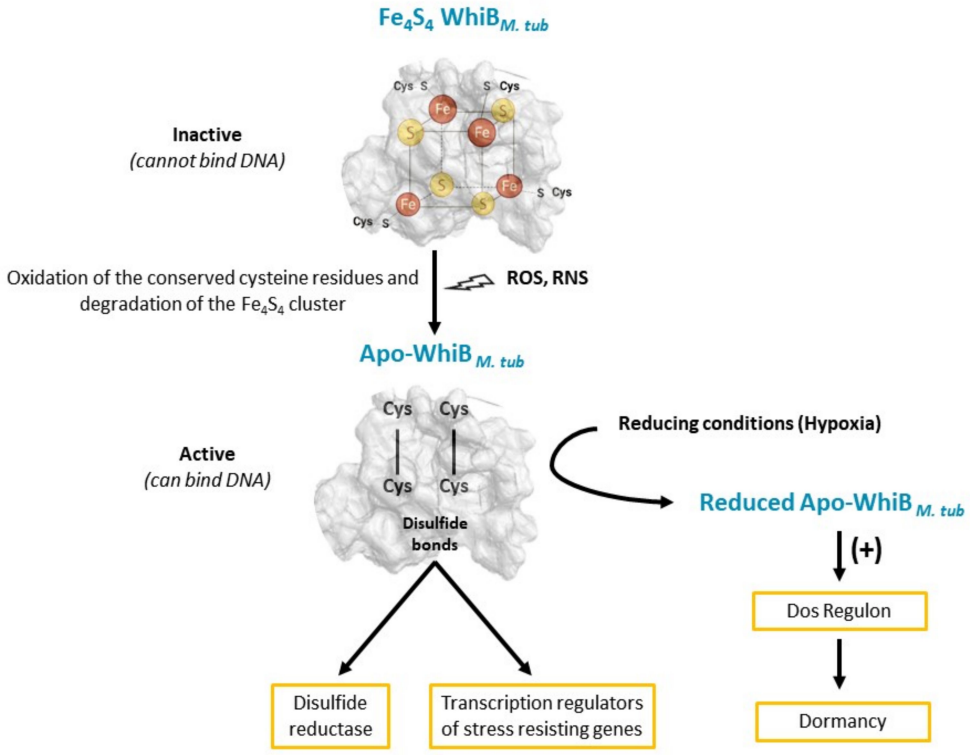

Figure 2. A scheme describing the role of the Fe-S cluster in *Mtb* WhiB proteins in sensing of extracellular stressors as ROS, NO, and hypoxic conditions. The holo-form of the WhiB containing an intact Fe-S cluster is unable to bind DNA, but when exposed to RNS or ROS, the conserved cysteine residues are oxidized and the Fe-S cluster degraded, leading to the apo-WhiB with disulfide bonds. All apo-forms of WhiB proteins, except WhiB2, display a disulfide reductase activity, and most of the apo-WhiB proteins are transcriptional regulators of stress-resisting genes. Under hypoxic conditions, apo-WhiB protein (WhiB6) becomes reduced, and under this form positively regulates the DOS regulon to prepare *Mtb* for dormancy [95].

4. How ROS, RNS and Fe Starvation Stresses Affect Iron-Sulfur (Fe-S) Cluster Proteins

We discussed previously (part 2) the different stresses which *Mtb* has to battle. Fe-S clusters are good targets for ROS and RNS and are susceptible to Fe starvation. Here, we will describe at a molecular level how these stresses can disrupt Fe-S clusters in bacteria. In some cases, the disruption is deleterious and leads to the inactivation of the protein

by breaking the cluster. In other cases, the cluster disrupted by the stress (leading to its degradation or its modification) is used as a sensor, as in the case of transcriptional regulators.

4.1. Fe-S Clusters Sensors of Reactive Oxygen Species

Fe_4S_4 clusters are sensitive to oxidative degradation, in particular solvent-accessible Fe_4S_4 clusters, and as such are used at times as sensors of oxidative stress. In E. coli, a well-known case is the fumarate and nitrate reductase FNR, a transcriptional regulator that controls the expression of a large regulon of more than 100 genes in response to changes in oxygen availability [96,97]. FNR is active when it acquires, under anaerobic conditions, a Fe_4S_4 cluster in the +2 oxidation state. The presence of this cluster per monomer promotes protein dimerization and site-specific DNA binding, facilitating activation or repression of target promoters in response to anaerobiosis [98,99]. FNR directly senses O_2 through the lability of its Fe_4S_4 cluster. As oxygen levels rise, the oxygen-labile Fe_4S_4 cluster of FNR is oxidized and converted to a variety of protein-bound clusters, including a $[Fe_3S_4]^{1+}$ and a $[Fe_2S_2]^{2+}$, along with an unexpected Fe_3S_3 cluster [100,101]. Conversion of the $[Fe_4S_4]^{2+}$ cluster to a lower cluster nuclearity presumably alters FNR's conformation, unable to bind DNA. Recent structural analysis of FNR from *Aliivibrio fischer* explained the extremely fine-tuned dimer–monomer equilibrium, giving insights into the DNA dissociation mechanism [102]. In *E. coli*, the redox-sensitive transcriptional regulator SoxR also responds to ROS. SoxR is activated under oxidative conditions by the oxidation of its $[Fe_2S_2]^{1+}$ cluster into the $[Fe_2S_2]^{2+}$ form [103,104]. The recent structure of SoxR from *E. coli* shows that the Fe_2S_2 is completely solvent-exposed, explaining how it can sense small molecules [105] such as superoxide or redox-cycling drugs such as paraquate, menadione and phenazine methosulfate [106]. Once the SoxR cluster is oxidized, SoxR activates the expression of SoxS, which in turn activates a large number of genes (superoxide dismutase, DNA repair nuclease, oxidation resistant enzymes), thereby restoring some essential cellular functions [107–110].

4.2. Fe-S Cluster Sensors of Reactive Nitrogen Species

The interaction of nitric oxide with Fe-S cluster proteins results in degradation and breakdown of the cluster to generate dinitrosyl iron complexes (DNICs). Like for oxidation of clusters, the formation of DNICs from Fe-S clusters can lead to activation of a regulatory pathway or the loss of enzyme activity. At low concentrations, NO is a signaling molecule that several bacterial proteins sense; among the Fe-S containing proteins, the best studied is the transcriptional regulator NsrR (nitric-oxide-sensitive response regulator) that functions as a regulator of NO-induced stress response in many bacterial species. In *E. coli*, $\geq$60 genes are under NsrR control, the principal target being the NO stress response (*hmp*, which encodes a flavohaemoglobin that converts NO to nitrate under aerobic conditions and *nrfA*) and general stress response (*sodB*) [111,112]. NsrR is an Fe_4S_4 protein [113] with a unique coordination of the cluster at the interface of the two subunits of a dimer, by three Cys residues of one subunit and an Asp residue of the other. In its Fe_4S_4 form, NsrR is able to bind DNA and thus represses the cell's response to NO stress. Upon exposure to NO, the cluster undergoes a rapid, complex, nitrosylation reaction resulting in the loss of DNA-binding (because of conformational change and/or change in affinity for target DNA) and the formation of a mixture of Fe-nitrosyl species [114]. SoxR and FNR are partially destroyed by NO [115,116], showing that they play a minor role as NO sensors.

4.3. The Case of Mtb WhiB Proteins

Mtb does not contain redox sensors such as SoxR, NsrR or FNR. Instead, *Mtb* contains WhiB proteins as transcriptional regulators, which sense NO and O_2 stresses. Of the seven WhiB-like proteins of *Mtb*, only WhiB1, WhiB3, WhiB4 and WhiB6 have been investigated at a molecular level. As mentioned before, the Fe_4S_4 clusters of WhiB proteins (for those which were characterized) have different sensitivity towards NO and ROS. WhiB1 expres-

sion is regulated by cAMP-CRP [117,118] (Figure 3). Under its holo-form (Fe_4S_4), WhiB1 cannot bind DNA; its cluster is stable to O_2 and remarkably sensitive to NO, reacting 10^4-fold faster than its reaction with O_2 [119]. During *Mtb* infection, the Fe_4S_4-WhiB1 protein detects NO in the microenvironment through its Fe_4S_4 cluster [119]; it reacts with eight NO molecules, leading to the cluster disassembly by nitrosylation, releasing the apo-WhiB1 and nitrosylated-WhiB1, able to bind specific DNA sequences, acting as a transcriptional regulator [120]. The nitrosylation and cluster degradation are thought to follow the following mechanism: $[Fe^{II}{}_2Fe^{III}{}_2S_4(Cys)_4]^{2-} + 8NO \rightarrow 2(Fe^{I}{}_2(Cys)_2(NO)_4) + S^{2-} + 3S^{\circ}$ [121]. The apo-form of WhiB1, as well as nitrosylated holo-WhiB1, bind to the whiB1 promoter region to repress its own transcription. In addition, WhiB1 regulates the secretion of ESX-1 [120] (a virulence factor that interrupts innate immune mechanisms) and represses transcription of groEL2 (an essential chaperonin), assisting entry into the dormant state of *Mtb* [122]. The apo-form of WhiB1 is also endowed with a disulfide reductase activity of the α(1,4)-glucan branching enzyme GlgB [123] and was reported to interact with the principal sigma factor SigA [124,125], which is essential for virulence in *Mtb* [126]. By similarity with other WhiB proteins, *Mtb* WhiB2 likely contains a Fe_4S_4 cluster, although its presence remains to be demonstrated. WhiB2 is regulated in response to antibiotics [127], and to ROS and heat-shock through SigB protein (Figure 3) [128–130]; a direct interaction between ROS and the WhiB2 cluster has not been reported. WhiB2 was recently reported to interact with SigA factor [124]. *Mtb* WhiB3 is positively regulated by PhoP [131] in response to acidic environments both in vitro and in macrophages [132,133], by phosphorylated RegX3 in response to low pH [134] and by MprAB through upregulation of Rv0081, predicted to induce the whiB3 operon [117]. WhiB3 harbors a Fe_4S_4 cluster that reacts with NO and slowly with O_2 [135], likely through the mechanism described above for WhiB1. Once the cluster is lost, cysteine residues, initially involved in Fe-S coordination, form intramolecular disulfide bonds that enable WhiB3 to interact strongly with DNA. Upon NO stress, WhiB3 induces lipid (polyketides, pks) production [136], which are responsible for arresting the host cell cycle of infected macrophages at the G_0/G_1 phase, thus manipulating the immune system [137], pathogenicity (through SigA interaction) [124,138] and lipid anabolism to modulate macrophage response (through fbpA, necessary for glycolipid trehalose dimycolate production) [136]. WhiB4 is over-expressed in the host macrophages and thus plays a role in the in vivo persistence. As-purified WhiB4 contains a Fe_2S_2 cluster, while after reconstitution it shields an Fe_4S_4 cluster [139]. Both Fe_2S_2 and Fe_4S_4 clusters are extremely NO- and O_2-sensitive [139,140]. The Fe_4S_4 cluster seems more sensitive to O_2 than those reported for other WhiB such as WhiB3 and WhiB1, suggesting a specific role of WhiB4 in redox sensing [140]. Holo-WhiB4 is not competent to bind to DNA, whereas apo-WhiB4 (with oxidized cysteines) binds strongly to DNA. Apo-WhiB4 binds to the promotor of ahpC, which encodes a protein responsive in suppressing oxidative stress [121]. The apo-form display also a disulfide reductase activity [140]. Like most of the WhiB proteins, WhiB4 interacts with SigA [124]. WhiB5 is regulated by oxidative stress and regulates the transcription of a number of genes, including sigM (alternative RNA polymerase sigma factor) and the genes for two type VII secretion systems, ESX-2 and ESX-4 [141]. The presence of an Fe-S cluster and the molecular mechanism in response to the oxidative stress remain to be discovered. When the Fe_4S_4-containing form of WhiB6 interacts with ROS and NO, the cluster undergoes degradation and the apo-WhiB6 and WhiB6-DNIC are formed, respectively [95]. WhiB6-DNIC suppresses ESX-1 expression, while WhiB6-DNIC and reduced apo-WhiB6 induce the DosR regulon in order to maintain the integrity of the granuloma and prepare the cell for latency [95]. WhiB6 also regulates the expression of espACD [95]. Like for WhiB2 and WhiB5, almost nothing is known regarding WhiB7, beyond its expression profile and its protein disulfide reductase activity [93]. It plays a role in antibiotics resistance [142]. WhiB7 is reported to be activated by oxidative stress, although the mechanism is not known. Like all WhiB proteins, it contains the four conserved cysteine residues that are able to bind the redox active Fe-S cluster, suggesting that it is also able to shield a Fe-S cluster. Recently, structural studies have demonstrated

the presence of a Fe_4S_4 cluster in WhiB7 [143]. WhiB7 was reported to regulate a significant number of genes, such as cut2, erm, hflX, tap, Rv0263, Rv1257c, Rv1988, and Rv1473 [144], and there are several evidences of its interaction with SigA [124,143,145,146]. In summary, unlike *E. coli*, which has specialized proteins to respond to O2 and NO stresses, *Mtb* relies on a single family of proteins, WhiB, to sense these stresses. Through WhiB proteins, one notices how Fe-S clusters are critical for *Mtb* virulence and persistence.

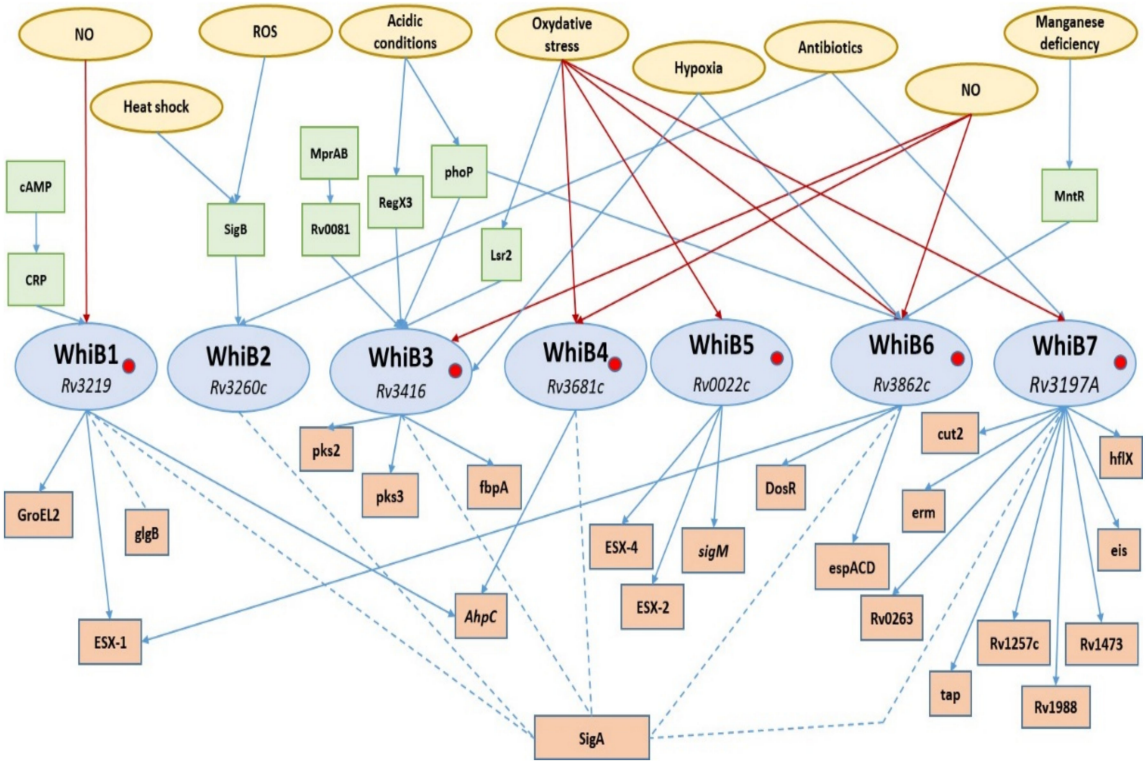

Figure 3. Regulation network of *Mtb* WhiB proteins. The red circle indicates that the protein displays a disulfide reductase activity. Blue arrows indicate regulation (up- or downregulation), while blue dashed lines indicate an interaction between WhiB proteins and SigA factor [124,125,138,146]. Red arrows focus on the WhiB proteins regulated by oxidative stress and NO.

4.4. Fe-S Enzymes and ROS/RNS

At high concentrations, or if conditions persist, ROS and NOS can be deleterious to Fe-S cluster enzymes; the resulting apo-enzyme may lead to protein degradation and cell death in case of essential enzymes. Sometimes, the apo-enzyme can be repaired by adding Fe^{2+} and a reducing agent [147]. Superoxide and hydrogen peroxide can inactivate Fe_4S_4 enzymes, including dehydratases and radical-SAM enzymes. The common point of these enzymes is their solvent-exposed Fe_4S_4 cluster; it is necessary for their function, but at the same time it endangers them. Many years ago, Fridovich and Flint discovered that superoxide rapidly inactivates the Fe_4S_4 family of dehydratases, including key enzymes of the branched-chain and TCA pathways (dehydratases, aconitase and fumarase and isopropylmalate isomerase) [148–150]. This is also true for α,β-dihydroisovalerate and dehydrogenase 3-Deoxy-D-Arabinoheptulosonate 7-Phosphate Synthase [22,151]. The damage occurs when superoxide directly oxidizes the Fe-S cluster, converting the $[Fe_4S_4]^{2+}$ form to an unstable $[Fe_4S_4]^{3+}$, which releases iron (Fe^{2+}). The resultant $[Fe_3S_4]^{1+}$ cluster lacks the catalytic iron atom, so that the enzyme is inactive and the pathway with which it is involved fails. Most of the time, the $[Fe_3S_4]^{1+}$ cluster is converted to $[Fe_2S_2]^{2+}$ that can be ultimately degraded. After exposure to air, the quinolinate synthase $[Fe_4S_4]^{2+}$ cluster is converted to a stable $[Fe_2S_2]^{2+}$ [152]. The rate constants with which dehydratase clusters react with superoxide and hydrogen peroxide are extremely high: 3×10^6 M^{-1} s^{-1} and

4×10^3 M^{-1} s^{-1}, respectively [153]. It is not surprising, as these oxidants are small and can enter the active sites of dehydratases which are solvent-exposed. SAM-superfamily enzymes—which use also a solvent exposed Fe_4S_4 cluster to bind SAM and/or substrate—are also rapidly inactivated when they are exposed to oxygen. In vitro spectroscopic studies on Fe_4S_4 enzymes exposed to air or titration with H_2O_2 indicate stable or semi-stable breakdown intermediates. The Fe_4S_4 cluster of MiaB from *Thermotoga maritima* degrades into an $[Fe_2S_2]^{2+}$ cluster [154]. An $[Fe_2S_2]^{2+}$ cluster with cysteine persulfides was also observed by X-ray crystall ography in HydE enzyme [155]. None of the Fe-S-containing enzymes in *Mtb* (Table 1) have been investigated upon exposure to ROS and/or NO at a molecular level, but we can hypothesize that similar degradation mechanisms occur and therefore that essential metabolic pathways involving Fe-S enzymes may be hampered.

4.5. Iron Starvation and Fe-S Clusters

Fe-S clusters are formed from iron (Fe^{2+} and/or Fe^{3+}) and inorganic sulfide. Therefore, iron starvation in bacteria has a direct impact on the Fe-S cluster biogenesis machineries (dedicated to assembling Fe-S clusters from L-cysteine and iron) [156–158]. Nevertheless, *Mtb* contains only the SUF system, which is functional under iron limitation (as discussed above). Whether this is due to higher affinity of the SUF components to small iron chelate or iron-binding proteins is not known yet. *Mtb* manages with this stress with the synthesis of mycobactin siderophore, which chelates ferric iron from host storage proteins in the phagosome [31].

5. Activation of *Mtb* Fe-S Biogenesis and Metabolism upon ROS, NO and Fe Starvation Stresses

Mtb alleviates ROS and RNS partially through Fe-S cluster proteins involved in redox sensing, gene regulation and DNA repair for persistence, such as WhiB regulators [132,135,136,140,159]. While these findings underscore the importance of Fe-S clusters in ensuring stress tolerance and survival of *Mtb*, what do we know about Fe-S biogenesis in the human pathogen *Mtb*?

In bacteria, three pathways for Fe-S cluster biogenesis and delivery have been identified: the ISC, NIF and SUF systems [160]. The ISC system is considered as the housekeeping system, SUF acts as a backup in stress conditions, and NIF is specialized in the maturation of nitrogenase in N_2-fixing bacteria. Although made of different components, these three systems facilitate Fe-S cluster biogenesis following the same basic principles: a cysteine desulfurase takes sulfur from L-cysteine and transfers it as a persulfide onto a scaffold protein, which also receives Fe^{2+} and electrons to build an Fe-S cluster that is then transferred to cellular apo-protein targets via carrier proteins (Figure 4) [160]. Whereas some bacteria such as *E. coli* contain several Fe-S biogenesis machineries (SUF and ISC), interestingly, some pathogens, such as *Staphylococcus aureus* and *Mtb*, contain only the SUF system as Fe-S assembly machinery (Figure 4) [5,161]. An iscS gene (cysteine desulfurase, Rv3025c) is present outside the *suf* locus but corresponds to a separate ORF, and it is not surrounded by other isc genes [5]. Therefore, the SUF machinery appears to be the primary Fe-S system in *Mtb*. Based on extensive work performed on the SUF system of *E. coli* (*sufABCDSE*), it is known that (i) the SufS-SufE complex provides sulfur from L-cysteine; (ii) the SufB-SufC-SufD complex acts as a scaffold for the assembly of Fe-S clusters, and that (iii) the SufA protein is a Fe-S transporter [162] (Figure 4). However, despite intensive studies, the nature and ligand of the Fe-S cluster on the *E. coli* $SufBC_2D$ complex is still unknown and mysterious. The SUF system from the Gram(+) *Bacillus subtilis* (sufCDSUB) is also well studied, in particular the SufS and SufU proteins, which are implicated in the sulfur production of L-cysteine. As-purified SufU contains one zinc ion per protein essential to enhance the cysteine desulfurase activity of SufS [163]. SufU from *B. subtilis* was also proposed as an Fe-S cluster containing protein after reconstitution, although the FeS-SufU cannot promote activation of the SufS cysteine desulfurase activity [164]. In this study, only the apo-SufU (no Zn, no Fe-S) can activate SufS, in striking contrast to Selbach's data [164].

The characterization of the SufB, SufC and SufD proteins, which likely form a complex based on *E. coli* data, suffers from SufB protein instability, preventing its function from being determined. Interestingly, the *E. coli* and *B. subtilis* SUF systems show a series of differences, from genetic organization to genetic composition, and were recently shown to exhibit different efficiency in maturing heterologous Fe-S targets [165,166]. In *Mtb*, the *suf* operon is composed of seven genes, namely Rv1460(*sufR*), Rv1461(*sufB*), Rv1462(*sufD*), Rv1463(*sufC*), Rv1464(*sufS*), Rv1465(*sufU*) and Rv1466(*sufT*). From its genetic composition, it more resembles the *B. subtilis* SUF system than that of the *E. coli* one, even though SUF from *Mtb* contains the additional sufT gene. *sufT* is not unique to *Mtb* or mycobacteria. Indeed, in prokaryotes, bioinformatics analysis revealed that 70% of genomes encoding SufBC also encoded a SufT, and 49% of these are associated with the *suf* operon [167]. In the last decade, *Mtb* SUF proteins have been poorly explored at a molecular level, but recently some exciting studies have been reported. The SufR homologue Rv1460 is a repressor of the *Mtb suf* operon. It contains, after purification, an Fe_2S_2 cluster, proposed to be coordinated by three cysteine residues (Cys203, C216, and C244) [168]. A recent study suggests that SufR contains instead a Fe_4S_4 cluster that is a sensor of NO to support persistence by reprogramming Fe-S cluster metabolism and the bioenergetics of *Mtb* [169]. SufT is proposed to act as an accessory factor in Fe-S biogenesis in *Mtb*, since it is dispensable for growth of *Mtb* under standard culture conditions, required under conditions of iron limitation [170], and SufT loss does not increase susceptibility to oxidative stress [170]. Very recently, *Mtb* SufT protein was shown to interact with SufS and SufU and to maintain the activity of Fe-S cluster proteins during normal growth conditions, and under environmental settings that enforce a high demand of Fe-S clusters [171]. Characterizations of *Mtb* SufS and SufU will certainly provide additional information and interesting insights into the sulfur production. SufB, SufC and SufD proteins from *Mtb* interact *in cellulo* [5]; however, the structural and functional characterization of these proteins remain also to be carried out in order to determine whether, like the *E. coli* $SufBC_2D$, they play a scaffold role.

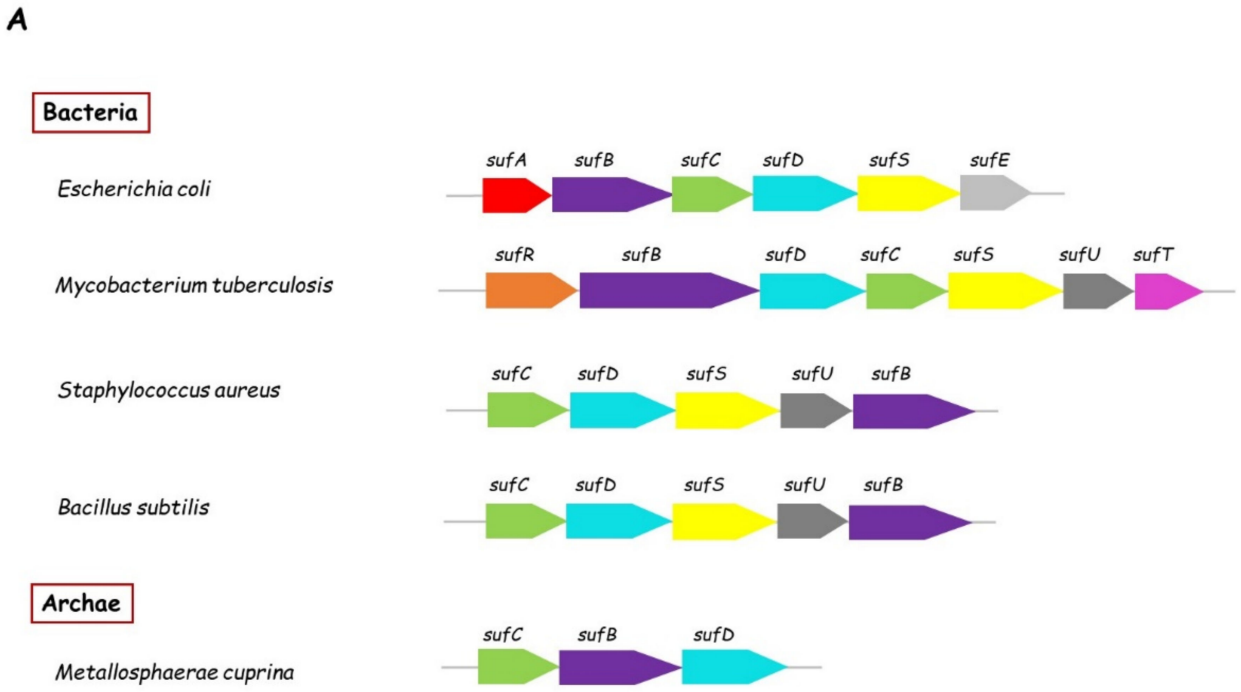

Figure 4. *Cont.*

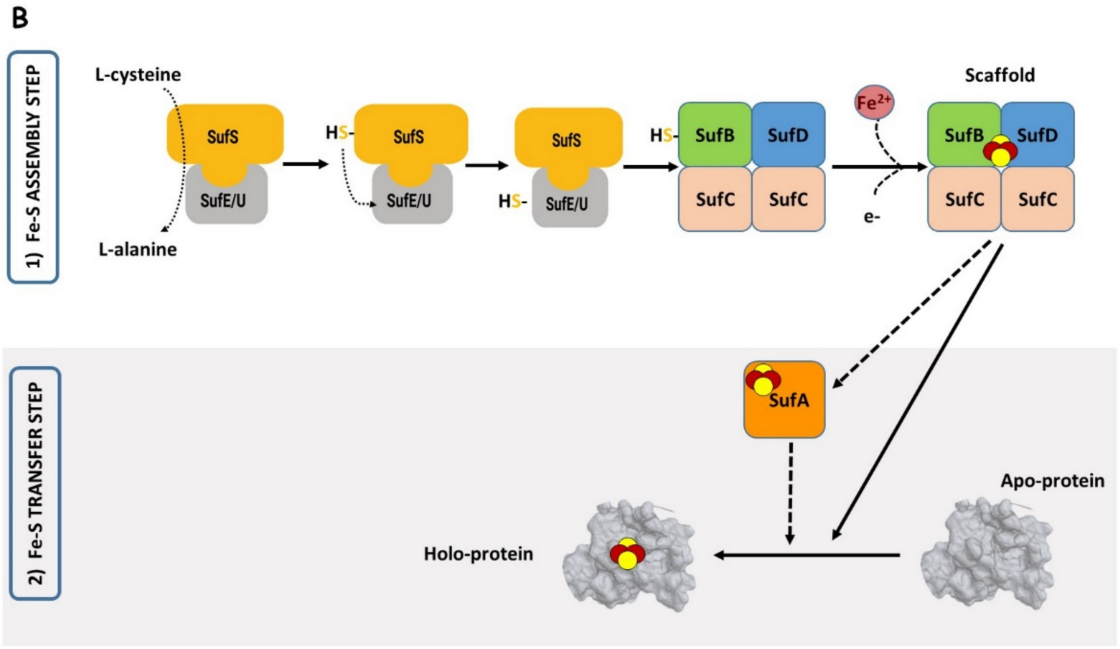

Figure 4. Organization and function of the SUF system. (**A**): genetic organization of *suf* operons in bacteria and archae. (**B**): role of the Suf proteins in Fe-S biogenesis (mainly from studies on *E. coli* and *B. subtilis* SUF systems).

Mtb suf operon is essential for the viability of *Mtb* under normal growth conditions [5,48,49]. More recently, Rv1461(*sufB*), Rv1462(*sufD*), Rv1463(*sufC*) and Rv1464(*sufS*) genes were proved to be vulnerable [52] (Table 2). The *Mtb suf* operon is under both transcriptional and post-translational regulation by SufR [168] and SufB, respectively, even though the mechanisms of these regulations are not well understood. SufR is involved in the regulation of the *Mtb suf* operon, acting as a transcriptional repressor of its own expression in *Mtb*, and also as a repressor of the *suf* operon [168]. The Fe-S cluster of Rv1460 is required for its function as cysteine-to-serine mutants alter SufR function. SufB from *Mtb* possesses an intein whose splicing appears to have a critical role in modulating interaction with SufC and SufD [172]. Recently, the *Mtb* SufB intein was shown to possess high sensitivity for oxidative and nitrosative stress when expressed in *E. coli* [173]. High levels of ROS and NO inhibit SufB splicing. The splicing inhibition is proposed to be an immediate, post-translational regulatory response that can be either reversible, by inducing precursor accumulation, or irreversible, by inducing N-terminal cleavage, which may potentially channel *Mtb* into dormancy under extreme NO and oxidative stress [173].

Table 2. Genes predicted to be implicated in Fe-S biogenesis in *Mtb* and their essentiality.

Essentiality Identification Method	Rv1460	Rv1461	Rv1462	Rv1463	Rv1464	Rv1465	Rv1466
Through transposon [47–50]	No	Yes	Yes	Yes	Yes	Yes	Yes
Through CRISPR interference/VI [52]	No VI: −3.9	Yes VI: −7.78	Yes VI: −7.60	Yes VI: −9.29	Yes VI: −5.38	No VI: −1.14	No? VI: 0.08

The *Mtb* Suf operon is upregulated under nitrosative (NO) and oxidative conditions (H_2O_2), stressors of the innate immune response [14,174]. Additionally, microarray-based expression profiles of the suf Fe-S cluster assembly genes show that Rv1460-Rv1466 genes are highly upregulated upon exposure to H_2O_2, NO, and within macrophages infection [3]. The upregulation of the *suf* operon is likely to compensate for the loss of Fe-S clusters due to oxidative stress in Fe-S enzymes such as aconitase, quinolinate synthase and other Fe-S enzymes. Moreover, *Mtb* SUF components are induced during iron starvation [175],

a process experienced by the pathogen in host tissues, indicating that Fe-S assembly and therefore Fe-S metabolism may be important in the establishment of latent infection. Intriguingly, suf genes are downregulated during hypoxia, a situation encountered in granulomas [3]. Therefore, interfering with Fe-S metabolism (SUF Fe-S biogenesis system) in *Mtb* offers a powerful strategy for eliminating TB (Figure 5). First, this will impose a pleiotropic effect on *Mtb*'s ability to synthesize the Fe-S proteins, some of which are essential in bioenergetics and central metabolism. Second, this will disarm *Mtb* by removing its ability to synthesize Fe-S for detecting environmental stress signals (through WhiB proteins). The loss (or inactivity) of the redox sensors WhiB would prevent the bacterium from mounting metabolic adaptations to enter a latent state. Importantly, the SUF system is absent in humans where Fe-S biogenesis is sustained by the ISC machinery [176]. Therefore, disrupting Fe-S cluster metabolism by targeting the *Mtb* SUF system is likely an exceptional route for developing novel anti-TB agents. So far, no inhibitors of the *Mtb* SUF machinery have been discovered.

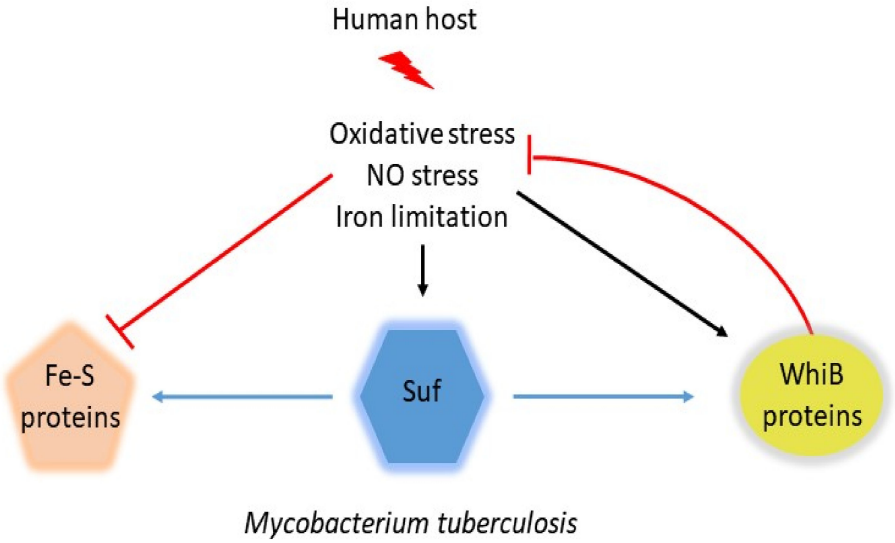

Figure 5. Importance of the SUF machinery in *Mtb* and its inhibition as a strategy to combat TB. The SUF system builds Fe-S clusters and transfers them to targets (Fe-S enzymes and WhiB proteins) (blue arrows). ROS and NO stresses encountered by *Mtb* in human host damage Fe-S clusters, inhibiting Fe-S enzymes (left red line). ROS and NO also damage Fe-S clusters of WhiB proteins that become active (black arrow) and then regulate expression of proteins to adjust *Mtb* metabolism to survive under stress conditions (right red line). ROS, NO and iron limitation stresses induce *suf* operon. Targeting the SUF system will disrupt Fe-S cluster metabolism: inability to maturate essential Fe-S enzymes and inability to detect environmental stress signals (WhiB proteins).

Author Contributions: Conceptualization, S.O.d.C., investigation, S.O.d.C., writing—original draft preparation, S.O.d.C., writing—review and editing, I.E., supervision, S.O.d.C., resources, S.O.d.C., I.E. All authors have read and agreed to the published version of the manuscript.

Funding: This work was supported by grants from the LabEx ARCANE (ANR-11-LABX-0003-01) and the CBH-EUR-GS (ANR-17-EURE-0003).

Institutional Review Board Statement: Not applicable.

Informed Consent Statement: Not applicable.

Data Availability Statement: The essentiality data (VI index) from Tables 1 and 2 are available as Supplementary Data (DataS2) in the reference [52].

Conflicts of Interest: The authors declare no conflict of interest.

References

1. World Health Organization. *Global Tuberculosis Report*; World Health Organization: Geneva, Switzerland, 2021. Available online: https://apps.who.int/iris/handle/10665/346387 (accessed on 25 August 2022).
2. Trivedi, A.; Singh, N.; Bhat, S.A.; Gupta, P.; Kumar, A. Redox biology of tuberculosis pathogenesis. *Adv. Microb. Physiol.* **2012**, *60*, 263–324. [PubMed]
3. Saini, V.; Farhana, A.; Glasgow, J.N.; Steyn, A.J. Iron sulfur cluster proteins and microbial regulation: Implications for understanding tuberculosis. *Curr. Opin. Chem. Biol.* **2012**, *16*, 45–53. [CrossRef] [PubMed]
4. Roche, B.; Aussel, L.; Ezraty, B.; Mandin, P.; Py, B.; Barras, F. Iron/sulfur proteins biogenesis in prokaryotes: Formation, regulation and diversity. *Biochim. Biophys. Acta* **2013**, *1827*, 455–469. [CrossRef]
5. Huet, G.; Daffe, M.; Saves, I. Identification of the Mycobacterium tuberculosis SUF machinery as the exclusive mycobacterial system of [Fe-S] cluster assembly: Evidence for its implication in the pathogen's survival. *J. Bacteriol.* **2005**, *187*, 6137–6146. [CrossRef] [PubMed]
6. Stallings, C.L.; Glickman, M.S. Is Mycobacterium tuberculosis stressed out? A critical assessment of the genetic evidence. *Microbes Infect.* **2010**, *12*, 1091–1101. [CrossRef]
7. Pacl, H.T.; Reddy, V.P.; Saini, V.; Chinta, K.C.; Steyn, A.J.C. Host-pathogen redox dynamics modulate Mycobacterium tuberculosis pathogenesis. *Pathog. Dis.* **2018**, *76*, fty036. [CrossRef]
8. Becker, K.; Sander, P. Mycobacterium tuberculosis lipoproteins in virulence and immunity—Fighting with a double-edged sword. *FEBS Lett.* **2016**, *590*, 3800–3819. [CrossRef]
9. Maitra, A.; Munshi, T.; Healy, J.; Martin, L.T.; Vollmer, W.; Keep, N.H.; Bhakta, S. Cell wall peptidoglycan in Mycobacterium tuberculosis: An Achilles' heel for the TB-causing pathogen. *FEMS Microbiol. Rev.* **2019**, *43*, 548–575. [CrossRef]
10. Yount, N.Y.; Yeaman, M.R. Peptide antimicrobials: Cell wall as a bacterial target. *Ann. N. Y. Acad. Sci.* **2013**, *1277*, 127–138. [CrossRef]
11. Armstrong, J.A.; Hart, P.D. Response of cultured macrophages to Mycobacterium tuberculosis, with observations on fusion of lysosomes with phagosomes. *J. Exp. Med.* **1971**, *134 Pt 1*, 713–740. [CrossRef]
12. Zhai, W.; Wu, F.; Zhang, Y.; Fu, Y.; Liu, Z. The Immune Escape Mechanisms of Mycobacterium Tuberculosis. *Int. J. Mol. Sci.* **2019**, *20*, 340. [CrossRef] [PubMed]
13. Pisu, D.; Huang, L.; Narang, V.; Theriault, M.; Le-Bury, G.; Lee, B.; Lakudzala, A.E.; Mzinza, D.T.; Mhango, D.V.; Mitini-Nkhoma, S.C.; et al. Single cell analysis of M. tuberculosis phenotype and macrophage lineages in the infected lung. *J. Exp. Med.* **2021**, *218*, e20210615. [CrossRef] [PubMed]
14. Voskuil, M.I.; Bartek, I.L.; Visconti, K.; Schoolnik, G.K. The response of mycobacterium tuberculosis to reactive oxygen and nitrogen species. *Front. Microbiol.* **2011**, *2*, 105. [CrossRef] [PubMed]
15. Flesch, I.E.; Kaufmann, S.H. Activation of tuberculostatic macrophage functions by gamma interferon, interleukin-4, and tumor necrosis factor. *Infect. Immun.* **1990**, *58*, 2675–2677. [CrossRef]
16. MacMicking, J.D.; North, R.J.; LaCourse, R.; Mudgett, J.S.; Shah, S.K.; Nathan, C.F. Identification of nitric oxide synthase as a protective locus against tuberculosis. *Proc. Natl. Acad. Sci. USA* **1997**, *94*, 5243–5248. [CrossRef]
17. Chan, J.; Xing, Y.; Magliozzo, R.S.; Bloom, B.R. Killing of Virulent Mycobacterium tuberculosis by Reactive Nitrogen Intermediates Produced by Activated Murine Macrophages. *J. Exp. Med.* **1992**, *175*, 1111–1122. [CrossRef]
18. Fang, F.C. Antimicrobial reactive oxygen and nitrogen species: Concepts and controversies. *Nat. Rev. Microbiol.* **2004**, *2*, 820–832. [CrossRef]
19. Gladwin, M.T.; Lancaster, J.R., Jr.; Freeman, B.A.; Schechter, A.N. Nitric oxide's reactions with hemoglobin: A view through the SNO-storm. *Nat. Med.* **2003**, *9*, 496–500. [CrossRef]
20. Russwurm, M.; Koesling, D. NO activation of guanylyl cyclase. *EMBO J.* **2004**, *23*, 4443–4450. [CrossRef]
21. Sarti, P.; Giuffre, A.; Forte, E.; Mastronicola, D.; Barone, M.C.; Brunori, M. Nitric oxide and cytochrome c oxidase: Mechanisms of inhibition and NO degradation. *Biochem. Biophys. Res. Commun.* **2000**, *274*, 183–187. [CrossRef]
22. Sobota, J.M.; Gu, M.; Imlay, J.A. Intracellular hydrogen peroxide and superoxide poison 3-deoxy-D-arabinoheptulosonate 7-phosphate synthase, the first committed enzyme in the aromatic biosynthetic pathway of Escherichia coli. *J. Bacteriol.* **2014**, *196*, 1980–1991. [CrossRef] [PubMed]
23. Imlay, J.A. Iron-sulphur clusters and the problem with oxygen. *Mol. Microbiol.* **2006**, *59*, 1073–1082. [CrossRef] [PubMed]
24. Jang, S.; Imlay, J.A. Micromolar intracellular hydrogen peroxide disrupts metabolism by damaging iron-sulfur enzymes. *J. Biol. Chem.* **2007**, *282*, 929–937. [CrossRef] [PubMed]
25. Kumar, R.; Subbian, S. Immune Correlates of Non-Necrotic and Necrotic Granulomas in Pulmonary Tuberculosis: A Pilot Study. *J. Respir.* **2021**, *4*, 248–259. [CrossRef]
26. Bange, F.C.; Brown, A.M.; Jacobs, W.R., Jr. Leucine auxotrophy restricts growth of Mycobacterium bovis BCG in macrophages. *Infect. Immun.* **1996**, *64*, 1794–1799. [CrossRef]
27. Hondalus, M.K.; Bardarov, S.; Russell, R.; Chan, J.; Jacobs, W.R., Jr.; Bloom, B.R. Attenuation of and protection induced by a leucine auxotroph of Mycobacterium tuberculosis. *Infect. Immun.* **2000**, *68*, 2888–2898. [CrossRef]
28. Rifat, D.; Bishai, W.R.; Karakousis, P.C. Phosphate depletion: A novel trigger for Mycobacterium tuberculosis persistence. *J. Infect. Dis.* **2009**, *200*, 1126–1135. [CrossRef]

29. Gordhan, B.G.; Smith, D.A.; Alderton, H.; McAdam, R.A.; Bancroft, G.J.; Mizrahi, V. Construction and phenotypic characterization of an auxotrophic mutant of Mycobacterium tuberculosis defective in L-arginine biosynthesis. *Infect. Immun.* **2002**, *70*, 3080–3084. [CrossRef]
30. Marcela Rodriguez, G.; Neyrolles, O. Metallobiology of Tuberculosis. *Microbiol. Spectr.* **2014**, *2*, 377–387. [CrossRef]
31. Sritharan, M. Iron Homeostasis in Mycobacterium tuberculosis: Mechanistic Insights into Siderophore-Mediated Iron Uptake. *J. Bacteriol.* **2016**, *198*, 2399–2409. [CrossRef]
32. Olakanmi, O.; Schlesinger, L.S.; Ahmed, A.; Britigan, B.E. Intraphagosomal Mycobacterium tuberculosis acquires iron from both extracellular transferrin and intracellular iron pools. Impact of interferon-gamma and hemochromatosis. *J. Biol. Chem.* **2002**, *277*, 49727–49734. [CrossRef] [PubMed]
33. Kaplan, G.; Post, F.A.; Moreira, A.L.; Wainwright, H.; Kreiswirth, B.N.; Tanverdi, M.; Mathema, B.; Ramaswamy, S.V.; Walther, G.; Steyn, L.M.; et al. Mycobacterium tuberculosis growth at the cavity surface: A microenvironment with failed immunity. *Infect. Immun.* **2003**, *71*, 7099–7108. [CrossRef] [PubMed]
34. Rustad, T.R.; Sherrid, A.M.; Minch, K.J.; Sherman, D.R. Hypoxia: A window into Mycobacterium tuberculosis latency. *Cell. Microbiol.* **2009**, *11*, 1151–1159. [CrossRef] [PubMed]
35. Beinert, H.; Sands, R.H. Studies on succinic and DPNH dehydrogenase preparations by paramagnetic resonance (EPR) spectroscopy. *Biochem. Biophys. Res. Commun.* **1960**, *3*, 41–46. [CrossRef]
36. Beinert, H. Recent developments in the field of iron-sulfur proteins. *FASEB J.* **1990**, *4*, 2483–2491. [CrossRef] [PubMed]
37. Beinert, H.; Holm, R.H.; Munck, E. Iron-sulfur clusters: Nature's modular, multipurpose structures. *Science* **1997**, *277*, 653–659. [CrossRef]
38. Meyer, J. Iron-sulfur protein folds, iron-sulfur chemistry, and evolution. *J. Biol. Inorg. Chem.* **2008**, *13*, 157–170. [CrossRef]
39. Hall, D.O.; Rao, K.K.; Cammack, R. The iron-sulphur proteins: Structure, function and evolution of a ubiquitous group of proteins. *Sci. Prog.* **1975**, *62*, 285–317.
40. Luchinat, C. Exchange versus double exchange in polymetallic Fe-S systems. *J. Biol. Inorg. Chem.* **1996**, *1*, 169–188.
41. Piccioli, M. The Biogenesis of Iron-sulfur Proteins: From Cellular Biology to Molecular Aspects. *J. Biol. Inorg. Chem.* **2018**, *23*, 599–687. [CrossRef]
42. Johnson, M.K.; Smith, A.D. Iron-Sulfur proteins. *Encycl. Inorg. Bioinorg. Chem.* **2011**. [CrossRef]
43. Johnson, D.C.; Dean, D.R.; Smith, A.D.; Johnson, M.K. Structure, function, and formation of biological iron-sulfur clusters. *Annu. Rev. Biochem.* **2005**, *74*, 247–281. [CrossRef] [PubMed]
44. Kiley, P.J.; Beinert, H. The role of Fe-S proteins in sensing and regulation in bacteria. *Curr. Opin. Microbiol.* **2003**, *6*, 181–185. [CrossRef]
45. Freibert, S.A.; Goldberg, A.V.; Hacker, C.; Molik, S.; Dean, P.; Williams, T.A.; Nakjang, S.; Long, S.; Sendra, K.; Bill, E.; et al. Evolutionary conservation and in vitro reconstitution of microsporidian iron-sulfur cluster biosynthesis. *Nat. Commun.* **2017**, *8*, 13932. [CrossRef]
46. Fontecave, M. Iron-sulfur clusters: Ever-expanding roles. *Nat. Chem. Biol.* **2006**, *2*, 171–174. [CrossRef]
47. DeJesus, M.A.; Gerrick, E.R.; Xu, W.; Park, S.W.; Long, J.E.; Boutte, C.C.; Rubin, E.J.; Schnappinger, D.; Ehrt, S.; Fortune, S.M.; et al. Comprehensive Essentiality Analysis of the Mycobacterium tuberculosis Genome via Saturating Transposon Mutagenesis. *Mbio* **2017**, *8*, e02133-16. [CrossRef]
48. Griffin, J.E.; Gawronski, J.D.; Dejesus, M.A.; Ioerger, T.R.; Akerley, B.J.; Sassetti, C.M. High-resolution phenotypic profiling defines genes essential for mycobacterial growth and cholesterol catabolism. *PLoS Pathog.* **2011**, *7*, e1002251. [CrossRef]
49. Sassetti, C.M.; Boyd, D.H.; Rubin, E.J. Genes required for mycobacterial growth defined by high density mutagenesis. *Mol. Microbiol.* **2003**, *48*, 77–84. [CrossRef]
50. Minato, Y.; Gohl, D.M.; Thiede, J.M.; Chacon, J.M.; Harcombe, W.R.; Maruyama, F.; Baughn, A.D. Genomewide Assessment of Mycobacterium tuberculosis Conditionally Essential Metabolic Pathways. *mSystems* **2019**, *4*, e00070-19. [CrossRef]
51. Lamichhane, G.; Zignol, M.; Blades, N.J.; Geiman, D.E.; Dougherty, A.; Grosset, J.; Broman, K.W.; Bishai, W.R. A postgenomic method for predicting essential genes at subsaturation levels of mutagenesis: Application to Mycobacterium tuberculosis. *Proc. Natl. Acad. Sci. USA* **2003**, *100*, 7213–7218. [CrossRef]
52. Bosch, B.; De Jesus, M.A.; Poulton, N.C.; Zhang, W.Z.; Engelhart, C.A.; Zaveri, A.; Lavalette, S.; Ruecker, N.; Trujillo, C.; Wallach, J.B.; et al. Genome-wide gene expression tuning reveals diverse vulnerabilities of M. tuberculosis. *Cell* **2021**, *184*, 4579–4592. [CrossRef] [PubMed]
53. Banerjee, S.; Nandyala, A.K.; Raviprasad, P.; Ahmed, N.; Hasnain, S.E. Iron-dependent RNA-binding activity of Mycobacterium tuberculosis aconitase. *J. Bacteriol.* **2007**, *189*, 4046–4052. [CrossRef] [PubMed]
54. Singh, V.; Chandra, D.; Srivastava, B.S.; Srivastava, R. Downregulation of Rv0189c, encoding a dihydroxyacid dehydratase, affects growth of Mycobacterium tuberculosis in vitro and in mice. *Microbiology* **2011**, *157 Pt 1*, 38–46. [CrossRef]
55. Bashiri, G.; Grove, T.L.; Hegde, S.S.; Lagautriere, T.; Gerfen, G.J.; Almo, S.C.; Squire, C.J.; Blanchard, J.S.; Baker, E.N. The active site of the Mycobacterium tuberculosis branched-chain amino acid biosynthesis enzyme dihydroxyacid dehydratase contains a 2Fe-2S cluster. *J. Biol. Chem.* **2019**, *294*, 13158–13170. [CrossRef] [PubMed]
56. Flint, D.H.; Emptage, M.H.; Finnegan, M.G.; Fu, W.; Johnson, M.K. The role and properties of the iron-sulfur cluster in Escherichia coli dihydroxy-acid dehydratase. *J. Biol. Chem.* **1993**, *268*, 14732–14742. [CrossRef]

57. McKnight, G.L.; Mudri, S.L.; Mathewes, S.L.; Traxinger, R.R.; Marshall, S.; Sheppard, P.O.; O'Hara, P.J. Molecular cloning, cDNA sequence, and bacterial expression of human glutamine:fructose-6-phosphate amidotransferase. *J. Biol. Chem.* **1992**, *267*, 25208–25212. [CrossRef]
58. Dailey, H.A.; Gerdes, S.; Dailey, T.A.; Burch, J.S.; Phillips, J.D. Noncanonical coproporphyrin-dependent bacterial heme biosynthesis pathway that does not use protoporphyrin. *Proc. Natl. Acad. Sci. USA* **2015**, *112*, 2210–2215. [CrossRef]
59. Dailey, T.A.; Dailey, H.A. Identification of [2Fe-2S] clusters in microbial ferrochelatases. *J. Bacteriol.* **2002**, *184*, 2460–2464. [CrossRef]
60. Smith, P.M.; Fox, J.L.; Winge, D.R. Biogenesis of the cytochrome bc(1) complex and role of assembly factors. *Biochim. Biophys. Acta* **2012**, *1817*, 276–286. [CrossRef]
61. Raman, K.; Yeturu, K.; Chandra, N. targetTB: A target identification pipeline for Mycobacterium tuberculosis through an interactome, reactome and genome-scale structural analysis. *BMC Syst. Biol.* **2008**, *2*, 109. [CrossRef]
62. Zhang, Y.; Morar, M.; Ealick, S.E. Structural biology of the purine biosynthetic pathway. *Cell Mol. Life Sci.* **2008**, *65*, 3699–3724. [CrossRef] [PubMed]
63. Grandoni, J.A.; Switzer, R.L.; Makaroff, C.A.; Zalkin, H. Evidence that the iron-sulfur cluster of Bacillus subtilis glutamine phosphoribosylpyrophosphate amidotransferase determines stability of the enzyme to degradation in vivo. *J. Biol. Chem.* **1989**, *264*, 6058–6064. [CrossRef]
64. Brown, A.C.; Eberl, M.; Crick, D.C.; Jomaa, H.; Parish, T. The nonmevalonate pathway of isoprenoid biosynthesis in Mycobacterium tuberculosis is essential and transcriptionally regulated by Dxs. *J. Bacteriol.* **2010**, *192*, 2424–2433. [CrossRef] [PubMed]
65. Miziorko, H.M. Enzymes of the mevalonate pathway of isoprenoid biosynthesis. *Arch. Biochem. Biophys.* **2011**, *505*, 131–143. [CrossRef] [PubMed]
66. Rekittke, I.; Wiesner, J.; Rohrich, R.; Demmer, U.; Warkentin, E.; Xu, W.; Troschke, K.; Hintz, M.; No, J.H.; Duin, E.C.; et al. Structure of (E)-4-hydroxy-3-methyl-but-2-enyl diphosphate reductase, the terminal enzyme of the non-mevalonate pathway. *J. Am. Chem. Soc.* **2008**, *130*, 17206–17207. [CrossRef] [PubMed]
67. Grawert, T.; Span, I.; Eisenreich, W.; Rohdich, F.; Eppinger, J.; Bacher, A.; Groll, M. Probing the reaction mechanism of IspH protein by x-ray structure analysis. *Proc. Natl. Acad. Sci. USA* **2010**, *107*, 1077–1081. [CrossRef]
68. Wang, K.; Wang, W.; No, J.H.; Zhang, Y.; Zhang, Y.; Oldfield, E. Inhibition of the Fe(4)S(4)-cluster-containing protein IspH (LytB): Electron paramagnetic resonance, metallacycles, and mechanisms. *J. Am. Chem. Soc.* **2010**, *132*, 6719–6727. [CrossRef]
69. Brown, A.C.; Kokoczka, R.; Parish, T. LytB1 and LytB2 of Mycobacterium tuberculosis Are Not Genetically Redundant. *PLoS ONE* **2015**, *10*, e0135638.
70. Wolff, M.; Seemann, M.; Tse Sum Bui, B.; Frapart, Y.; Tritsch, D.; Garcia Estrabot, A.; Rodriguez-Concepcion, M.; Boronat, A.; Marquet, A.; Rohmer, M. Isoprenoid biosynthesis via the methylerythritol phosphate pathway: The (E)-4-hydroxy-3-methylbut-2-enyl diphosphate reductase (LytB/IspH) from Escherichia coli is a [4Fe-4S] protein. *FEBS Lett.* **2003**, *541*, 115–120. [CrossRef]
71. Morris, T.W.; Reed, K.E.; Cronan, J.E., Jr. Identification of the gene encoding lipoate-protein ligase A of Escherichia coli. Molecular cloning and characterization of the lplA gene and gene product. *J. Biol. Chem.* **1994**, *269*, 16091–16100. [CrossRef]
72. Ma, Q.; Zhao, X.; Nasser Eddine, A.; Geerlof, A.; Li, X.; Cronan, J.E.; Kaufmann, S.H.; Wilmanns, M. The Mycobacterium tuberculosis LipB enzyme functions as a cysteine/lysine dyad acyltransferase. *Proc. Natl. Acad. Sci. USA* **2006**, *103*, 8662–8667. [CrossRef] [PubMed]
73. Cicchillo, R.M.; Lee, K.H.; Baleanu-Gogonea, C.; Nesbitt, N.M.; Krebs, C.; Booker, S.J. Escherichia coli lipoyl synthase binds two distinct [4Fe-4S] clusters per polypeptide. *Biochemistry* **2004**, *43*, 11770–11781. [CrossRef] [PubMed]
74. Harmer, J.E.; Hiscox, M.J.; Dinis, P.C.; Fox, S.J.; Iliopoulos, A.; Hussey, J.E.; Sandy, J.; Van Beek, F.T.; Essex, J.W.; Roach, P.L. Structures of lipoyl synthase reveal a compact active site for controlling sequential sulfur insertion reactions. *Biochem. J.* **2014**, *464*, 123–133. [CrossRef] [PubMed]
75. McLaughlin, M.I.; Lanz, N.D.; Goldman, P.J.; Lee, K.H.; Booker, S.J.; Drennan, C.L. Crystallographic snapshots of sulfur insertion by lipoyl synthase. *Proc. Natl. Acad. Sci. USA* **2016**, *113*, 9446–9450. [CrossRef] [PubMed]
76. Lanz, N.D.; Lee, K.H.; Horstmann, A.K.; Pandelia, M.E.; Cicchillo, R.M.; Krebs, C.; Booker, S.J. Characterization of Lipoyl Synthase from Mycobacterium tuberculosis. *Biochemistry* **2016**, *55*, 1372–1383. [CrossRef]
77. Jurgenson, C.T.; Begley, T.P.; Ealick, S.E. The structural and biochemical foundations of thiamin biosynthesis. *Annu. Rev. Biochem.* **2009**, *78*, 569–603. [CrossRef]
78. Chatterjee, A.; Li, Y.; Zhang, Y.; Grove, T.L.; Lee, M.; Krebs, C.; Booker, S.J.; Begley, T.P.; Ealick, S.E. Reconstitution of ThiC in thiamine pyrimidine biosynthesis expands the radical SAM superfamily. *Nat. Chem. Biol.* **2008**, *4*, 758–765. [CrossRef]
79. Martinez-Gomez, N.C.; Downs, D.M. ThiC is an [Fe-S] cluster protein that requires AdoMet to generate the 4-amino-5-hydroxymethyl-2-methylpyrimidine moiety in thiamin synthesis. *Biochemistry* **2008**, *47*, 9054–9056. [CrossRef]
80. Fenwick, M.K.; Mehta, A.P.; Zhang, Y.; Abdelwahed, S.H.; Begley, T.P.; Ealick, S.E. Non-canonical active site architecture of the radical SAM thiamin pyrimidine synthase. *Nat. Commun.* **2015**, *6*, 6480. [CrossRef]
81. Szekely, R.; Rengifo-Gonzalez, M.; Singh, V.; Riabova, O.; Benjak, A.; Piton, J.; Cimino, M.; Kornobis, E.; Mizrahi, V.; Johnsson, K.; et al. 6,11-Dioxobenzo[f]pyrido [1,2-a]indoles Kill Mycobacterium tuberculosis by Targeting Iron-Sulfur Protein Rv0338c (IspQ), A Putative Redox Sensor. *ACS Infect. Dis.* **2020**, *6*, 3015–3025. [CrossRef]

82. van den Heuvel, R.H.; Curti, B.; Vanoni, M.A.; Mattevi, A. Glutamate synthase: A fascinating pathway from L-glutamine to L-glutamate. *Cell. Mol. Life Sci.* **2004**, *61*, 669–681. [CrossRef] [PubMed]
83. Vanoni, M.A.; Dossena, L.; van den Heuvel, R.H.; Curti, B. Structure-function studies on the complex iron-sulfur flavoprotein glutamate synthase: The key enzyme of ammonia assimilation. *Photosynth. Res.* **2005**, *83*, 219–238. [CrossRef] [PubMed]
84. Cheung, Y.W.; Tanner, J.A. Targeting glutamate synthase for tuberculosis drug development. *Hong Kong Med. J.* **2011**, *17* (Suppl. 2), 32–34. [PubMed]
85. Cherrier, M.V.; Chan, A.; Darnault, C.; Reichmann, D.; Amara, P.; Ollagnier de Choudens, S.; Fontecilla-Camps, J.C. The crystal structure of Fe(4)S(4) quinolinate synthase unravels an enzymatic dehydration mechanism that uses tyrosine and a hydrolase-type triad. *J. Am. Chem. Soc.* **2014**, *136*, 5253–5256. [CrossRef]
86. Rousset, C.; Fontecave, M.; Ollagnier de Choudens, S. The [4Fe-4S] cluster of quinolinate synthase from Escherichia coli: Investigation of cluster ligands. *FEBS Lett.* **2008**, *582*, 2937–2944. [CrossRef]
87. Rousset, C. *Etude Structurale et Fonctionnelle de la Quinolinate Synthase: Une Protéine Fersoufre Cible D'agents Antibactériens. Biochimie [q-bio.BM]*; Université Joseph-Fourier: Grenoble, France, 2009.
88. Reichmann, D.; Coute, Y.; Ollagnier de Choudens, S. Dual activity of quinolinate synthase: Triose phosphate isomerase and dehydration activities play together to form quinolinate. *Biochemistry* **2015**, *54*, 6443–6446. [CrossRef]
89. Volbeda, A.; Cabodevilla, J.S.; Darnault, C.; Gigarel, O.; Han, T.H.L.; Renoux, O.; Hamelin, O.; Agnier-de-Choudens, S.; Amara, P.; Fontecilla-Camps, J.C. Crystallographic Trapping of Reaction Intermediates in Quinolinic Acid Synthesis by NadA. *Acs Chem. Biol.* **2018**, *13*, 1209–1217. [CrossRef]
90. Volbeda, A.; Darnault, C.; Renoux, O.; Reichmann, D.; Amara, P.; Ollagnier de Choudens, S.; Fontecilla-Camps, J.C. Crystal Structures of Quinolinate Synthase in Complex with a Substrate Analogue, the Condensation Intermediate, and Substrate-Derived Product. *J. Am. Chem. Soc.* **2016**, *138*, 11802–11809. [CrossRef]
91. Saez Cabodevilla, J.; Volbeda, A.; Hamelin, O.; Latour, J.M.; Gigarel, O.; Clemancey, M.; Darnault, C.; Reichmann, D.; Amara, P.; Fontecilla-Camps, J.C.; et al. Design of specific inhibitors of quinolinate synthase based on [4Fe-4S] cluster coordination. *Chem. Commun.* **2019**, *55*, 3725–3728. [CrossRef]
92. Chan, A.; Clemancey, M.; Mouesca, J.M.; Amara, P.; Hamelin, O.; Latour, J.M.; Ollagnier de Choudens, S. Studies of inhibitor binding to the [4Fe-4S] cluster of quinolinate synthase. *Angew. Chem. Int. Ed. Engl.* **2012**, *51*, 7711–7714. [CrossRef]
93. Bush, M.J. The actinobacterial WhiB-like (Wbl) family of transcription factors. *Mol. Microbiol.* **2018**, *110*, 663–676. [CrossRef] [PubMed]
94. Alam, M.S.; Garg, S.K.; Agrawal, P. Studies on structural and functional divergence among seven WhiB proteins of Mycobacterium tuberculosis H37Rv. *FEBS J.* **2009**, *276*, 76–93. [CrossRef] [PubMed]
95. Chen, Z.; Hu, Y.; Cumming, B.M.; Lu, P.; Feng, L.; Deng, J.; Steyn, A.J.; Chen, S. Mycobacterial WhiB6 Differentially Regulates ESX-1 and the Dos Regulon to Modulate Granuloma Formation and Virulence in Zebrafish. *Cell Rep.* **2016**, *16*, 2512–2524. [CrossRef] [PubMed]
96. Kang, Y.; Weber, K.D.; Qiu, Y.; Kiley, P.J.; Blattner, F.R. Genome-wide expression analysis indicates that FNR of Escherichia coli K-12 regulates a large number of genes of unknown function. *J. Bacteriol.* **2005**, *187*, 1135–1160. [CrossRef]
97. Grainger, D.C.; Aiba, H.; Hurd, D.; Browning, D.F.; Busby, S.J. Transcription factor distribution in Escherichia coli: Studies with FNR protein. *Nucleic Acids Res.* **2007**, *35*, 269–278. [CrossRef]
98. Lazazzera, B.A.; Beinert, H.; Khoroshilova, N.; Kennedy, M.C.; Kiley, P.J. DNA binding and dimerization of the Fe-S-containing FNR protein from Escherichia coli are regulated by oxygen. *J. Biol. Chem.* **1996**, *271*, 2762–2768. [CrossRef]
99. Khoroshilova, N.; Popescu, C.; Munck, E.; Beinert, H.; Kiley, P.J. Iron-sulfur cluster disassembly in the FNR protein of Escherichia coli by O2: [4Fe-4S] to [2Fe-2S] conversion with loss of biological activity. *Proc. Natl. Acad. Sci. USA* **1997**, *94*, 6087–6092. [CrossRef]
100. Jervis, A.J.; Crack, J.C.; White, G.; Artymiuk, P.J.; Cheesman, M.R.; Thomson, A.J.; Le Brun, N.E.; Green, J. The O2 sensitivity of the transcription factor FNR is controlled by Ser24 modulating the kinetics of [4Fe-4S] to [2Fe-2S] conversion. *Proc. Natl. Acad. Sci. USA* **2009**, *106*, 4659–4664. [CrossRef]
101. Crack, J.C.; Green, J.; Cheesman, M.R.; Le Brun, N.E.; Thomson, A.J. Superoxide-mediated amplification of the oxygen-induced switch from [4Fe-4S] to [2Fe-2S] clusters in the transcriptional regulator FNR. *Proc. Natl. Acad. Sci. USA* **2007**, *104*, 2092–2097. [CrossRef]
102. Volbeda, A.; Darnault, C.; Renoux, O.; Nicolet, Y.; Fontecilla-Camps, J.C. The crystal structure of the global anaerobic transcriptional regulator FNR explains its extremely fine-tuned monomer-dimer equilibrium. *Sci. Adv.* **2015**, *1*, e1501086. [CrossRef]
103. Kobayashi, K.; Mizuno, M.; Fujikawa, M.; Mizutani, Y. Protein conformational changes of the oxidative stress sensor, SoxR, upon redox changes of the [2Fe-2S] cluster probed with ultraviolet resonance Raman spectroscopy. *Biochemistry* **2011**, *50*, 9468–9474. [CrossRef] [PubMed]
104. Hidalgo, E.; Ding, H.; Demple, B. Redox signal transduction: Mutations shifting [2Fe-2S] centers of the SoxR sensor-regulator to the oxidized form. *Cell* **1997**, *88*, 121–129. [CrossRef]
105. Watanabe, S.; Kita, A.; Kobayashi, K.; Miki, K. Crystal structure of the [2Fe-2S] oxidative-stress sensor SoxR bound to DNA. *Proc. Natl. Acad. Sci. USA* **2008**, *105*, 4121–4126. [CrossRef]
106. Gu, M.; Imlay, J.A. The SoxRS response of Escherichia coli is directly activated by redox-cycling drugs rather than by superoxide. *Mol. Microbiol.* **2011**, *79*, 1136–1150. [CrossRef] [PubMed]

107. Gaudu, P.; Weiss, B. SoxR, a [2Fe-2S] transcription factor, is active only in its oxidized form. *Proc. Natl. Acad. Sci. USA* **1996**, *93*, 10094–10098. [CrossRef]
108. Gaudu, P.; Moon, N.; Weiss, B. Regulation of the soxRS oxidative stress regulon. Reversible oxidation of the Fe-S centers of SoxR in vivo. *J. Biol. Chem.* **1997**, *272*, 5082–5086. [CrossRef]
109. Ding, H.; Demple, B. In vivo kinetics of a redox-regulated transcriptional switch. *Proc. Natl. Acad. Sci. USA* **1997**, *94*, 8445–8449. [CrossRef]
110. Pomposiello, P.J.; Bennik, M.H.; Demple, B. Genome-wide transcriptional profiling of the Escherichia coli responses to superoxide stress and sodium salicylate. *J. Bacteriol.* **2001**, *183*, 3890–3902. [CrossRef]
111. Efromovich, S.; Grainger, D.; Bodenmiller, D.; Spiro, S. Genome-wide identification of binding sites for the nitric oxide-sensitive transcriptional regulator NsrR. *Methods Enzymol.* **2008**, *437*, 211–233.
112. Partridge, J.D.; Bodenmiller, D.M.; Humphrys, M.S.; Spiro, S. NsrR targets in the Escherichia coli genome: New insights into DNA sequence requirements for binding and a role for NsrR in the regulation of motility. *Mol. Microbiol.* **2009**, *73*, 680–694. [CrossRef]
113. Volbeda, A.; Dodd, E.L.; Darnault, C.; Crack, J.C.; Renoux, O.; Hutchings, M.I.; Le Brun, N.E.; Fontecilla-Camps, J.C. Crystal structures of the NO sensor NsrR reveal how its iron-sulfur cluster modulates DNA binding. *Nat. Commun.* **2017**, *8*, 15052. [CrossRef] [PubMed]
114. Crack, J.C.; Gray, E.; Le Brun, N.E. Sensing mechanisms of iron-sulfur cluster regulatory proteins elucidated using native mass spectrometry. *Dalton Trans.* **2021**, *50*, 7887–7897. [CrossRef] [PubMed]
115. Lo, F.C.; Chen, C.L.; Lee, C.M.; Tsai, M.C.; Lu, T.T.; Liaw, W.F.; Yu, S.S. A study of NO trafficking from dinitrosyl-iron complexes to the recombinant E. coli transcriptional factor SoxR. *J. Biol. Inorg. Chem.* **2008**, *13*, 961–972. [CrossRef] [PubMed]
116. Crack, J.C.; Le Brun, N.E.; Thomson, A.J.; Green, J.; Jervis, A.J. Reactions of nitric oxide and oxygen with the regulator of fumarate and nitrate reduction, a global transcriptional regulator, during anaerobic growth of Escherichia coli. *Methods Enzymol.* **2008**, *437*, 191–209.
117. Zondervan, N.A.; van Dam, J.C.J.; Schaap, P.J.; Martins Dos Santos, V.A.P.; Suarez-Diez, M. Regulation of Three Virulence Strategies of Mycobacterium tuberculosis: A Success Story. *Int. J. Mol. Sci.* **2018**, *19*, 347. [CrossRef]
118. Stapleton, M.; Haq, I.; Hunt, D.M.; Arnvig, K.B.; Artymiuk, P.J.; Buxton, R.S.; Green, J. Mycobacterium tuberculosis cAMP receptor protein (Rv3676) differs from the Escherichia coli paradigm in its cAMP binding and DNA binding properties and transcription activation properties. *J. Biol. Chem.* **2010**, *285*, 7016–7027. [CrossRef]
119. Crack, J.C.; Smith, L.J.; Stapleton, M.R.; Peck, J.; Watmough, N.J.; Buttner, M.J.; Buxton, R.S.; Green, J.; Oganesyan, V.S.; Thomson, A.J.; et al. Mechanistic insight into the nitrosylation of the [4Fe-4S] cluster of WhiB-like proteins. *J. Am. Chem. Soc.* **2011**, *133*, 1112–1121. [CrossRef]
120. Kudhair, B.K.; Hounslow, A.M.; Rolfe, M.D.; Crack, J.C.; Hunt, D.M.; Buxton, R.S.; Smith, L.J.; Le Brun, N.E.; Williamson, M.P.; Green, J. Structure of a Wbl protein and implications for NO sensing by M. tuberculosis. *Nat. Commun.* **2017**, *8*, 2280. [CrossRef]
121. Chim, N.; Johnson, P.M.; Goulding, C.W. Insights into redox sensing metalloproteins in Mycobacterium tuberculosis. *J. Inorg. Biochem.* **2014**, *133*, 118–126. [CrossRef]
122. Stapleton, M.R.; Smith, L.J.; Hunt, D.M.; Buxton, R.S.; Green, J. Mycobacterium tuberculosis WhiB1 represses transcription of the essential chaperonin GroEL2. *Tuberculosis* **2012**, *92*, 328–332. [CrossRef]
123. Garg, S.K.; Suhail Alam, M.; Soni, V.; Radha Kishan, K.V.; Agrawal, P. Characterization of Mycobacterium tuberculosis WhiB1/Rv3219 as a protein disulfide reductase. *Protein Expr. Purif.* **2007**, *52*, 422–432. [CrossRef]
124. Feng, L.; Chen, Z.; Wang, Z.; Hu, Y.; Chen, S. Genome-wide characterization of monomeric transcriptional regulators in Mycobacterium tuberculosis. *Microbiology* **2016**, *162*, 889–897. [CrossRef] [PubMed]
125. Wan, T.; Li, S.; Beltran, D.G.; Schacht, A.; Zhang, L.; Becker, D.F.; Zhang, L. Structural basis of non-canonical transcriptional regulation by the sigmaA-bound iron-sulfur protein WhiB1 in M. tuberculosis. *Nucleic Acids Res.* **2020**, *48*, 501–516. [CrossRef] [PubMed]
126. Collins, D.M.; Kawakami, R.P.; de Lisle, G.W.; Pascopella, L.; Bloom, B.R.; Jacobs, W.R., Jr. Mutation of the principal sigma factor causes loss of virulence in a strain of the Mycobacterium tuberculosis complex. *Proc. Natl. Acad. Sci. USA* **1995**, *92*, 8036–8040. [CrossRef] [PubMed]
127. Geiman, D.E.; Raghunand, T.R.; Agarwal, N.; Bishai, W.R. Differential gene expression in response to exposure to antimycobacterial agents and other stress conditions among seven Mycobacterium tuberculosis whiB-like genes. *Antimicrob. Agents Chemother.* **2006**, *50*, 2836–2841. [CrossRef]
128. Lee, J.H.; Karakousis, P.C.; Bishai, W.R. Roles of SigB and SigF in the Mycobacterium tuberculosis sigma factor network. *J. Bacteriol.* **2008**, *190*, 699–707. [CrossRef]
129. Manganelli, R.; Dubnau, E.; Tyagi, S.; Kramer, F.R.; Smith, I. Differential expression of 10 sigma factor genes in Mycobacterium tuberculosis. *Mol. Microbiol.* **1999**, *31*, 715–724. [CrossRef]
130. Hurst-Hess, K.; Biswas, R.; Yang, Y.; Rudra, P.; Lasek-Nesselquist, E.; Ghosh, P. Mycobacterial SigA and SigB Cotranscribe Essential Housekeeping Genes during Exponential Growth. *Mbio* **2019**, *10*, e00273-19. [CrossRef]
131. Feng, L.; Chen, S.; Hu, Y. PhoPR Positively Regulates whiB3 Expression in Response to Low pH in Pathogenic Mycobacteria. *J. Bacteriol.* **2018**, *200*, e00766-17. [CrossRef]
132. Mehta, M.; Rajmani, R.S.; Singh, A. Mycobacterium tuberculosis WhiB3 Responds to Vacuolar pH-induced Changes in Mycothiol Redox Potential to Modulate Phagosomal Maturation and Virulence. *J. Biol. Chem.* **2016**, *291*, 2888–2903. [CrossRef]

133. Zheng, F.; Long, Q.; Xie, J. The function and regulatory network of WhiB and WhiB-like protein from comparative genomics and systems biology perspectives. *Cell. Biochem. Biophys.* **2012**, *63*, 103–108. [CrossRef] [PubMed]
134. Mahatha, A.C.; Mal, S.; Majumder, D.; Saha, S.; Ghosh, A.; Basu, J.; Kundu, M. RegX3 Activates whiB3 Under Acid Stress and Subverts Lysosomal Trafficking of Mycobacterium tuberculosis in a WhiB3-Dependent Manner. *Front. Microbiol.* **2020**, *11*, 572433. [CrossRef]
135. Singh, A.; Guidry, L.; Narasimhulu, K.V.; Mai, D.; Trombley, J.; Redding, K.E.; Giles, G.I.; Lancaster, J.R., Jr.; Steyn, A.J. Mycobacterium tuberculosis WhiB3 responds to O2 and nitric oxide via its [4Fe-4S] cluster and is essential for nutrient starvation survival. *Proc. Natl. Acad. Sci. USA* **2007**, *104*, 11562–11567. [CrossRef] [PubMed]
136. Singh, A.; Crossman, D.K.; Mai, D.; Guidry, L.; Voskuil, M.I.; Renfrow, M.B.; Steyn, A.J. Mycobacterium tuberculosis WhiB3 maintains redox homeostasis by regulating virulence lipid anabolism to modulate macrophage response. *PLoS Pathog.* **2009**, *5*, e1000545. [CrossRef]
137. Cumming, B.M.; Rahman, M.A.; Lamprecht, D.A.; Rohde, K.H.; Saini, V.; Adamson, J.H.; Russell, D.G.; Steyn, A.J.C. Mycobacterium tuberculosis arrests host cycle at the G1/S transition to establish long term infection. *PLoS Pathog.* **2017**, *13*, e1006389.
138. Steyn, A.J.; Collins, D.M.; Hondalus, M.K.; Jacobs, W.R., Jr.; Kawakami, R.P.; Bloom, B.R. Mycobacterium tuberculosis WhiB3 interacts with RpoV to affect host survival but is dispensable for in vivo growth. *Proc. Natl. Acad. Sci. USA* **2002**, *99*, 3147–3152. [CrossRef]
139. Alam, M.S.; Garg, S.K.; Agrawal, P. Molecular function of WhiB4/Rv3681c of Mycobacterium tuberculosis H37Rv: A [4Fe-4S] cluster co-ordinating protein disulphide reductase. *Mol. Microbiol.* **2007**, *63*, 1414–1431. [CrossRef]
140. Chawla, M.; Parikh, P.; Saxena, A.; Munshi, M.; Mehta, M.; Mai, D.; Srivastava, A.K.; Narasimhulu, K.V.; Redding, K.E.; Vashi, N.; et al. Mycobacterium tuberculosis WhiB4 regulates oxidative stress response to modulate survival and dissemination in vivo. *Mol. Microbiol.* **2012**, *85*, 1148–1165. [CrossRef]
141. Casonato, S.; Cervantes Sanchez, A.; Haruki, H.; Rengifo Gonzalez, M.; Provvedi, R.; Dainese, E.; Jaouen, T.; Gola, S.; Bini, E.; Vicente, M.; et al. WhiB5, a transcriptional regulator that contributes to Mycobacterium tuberculosis virulence and reactivation. *Infect. Immun.* **2012**, *80*, 3132–3144. [CrossRef]
142. Ramon-Garcia, S.; Ng, C.; Jensen, P.R.; Dosanjh, M.; Burian, J.; Morris, R.P.; Folcher, M.; Eltis, L.D.; Grzesiek, S.; Nguyen, L.; et al. WhiB7, an Fe-S-dependent transcription factor that activates species-specific repertoires of drug resistance determinants in actinobacteria. *J. Biol. Chem.* **2013**, *288*, 34514–34528. [CrossRef]
143. Wan, T.; Horova, M.; Beltran, D.G.; Li, S.; Wong, H.X.; Zhang, L.M. Structural insights into the functional divergence of WhiB-like proteins in Mycobacterium tuberculosis. *Mol. Cell.* **2021**, *81*, 2887–2900.e5. [CrossRef] [PubMed]
144. Morris, R.P.; Nguyen, L.; Gatfield, J.; Visconti, K.; Nguyen, K.; Schnappinger, D.; Ehrt, S.; Liu, Y.; Heifets, L.; Pieters, J.; et al. Ancestral antibiotic resistance in Mycobacterium tuberculosis. *Proc. Natl. Acad. Sci. USA* **2005**, *102*, 12200–12205. [CrossRef] [PubMed]
145. Lilic, M.; Darst, S.A.; Campbell, E.A. Structural basis of transcriptional activation by the Mycobacterium tuberculosis intrinsic antibiotic-resistance transcription factor WhiB7. *Mol. Cell.* **2021**, *81*, 2875–2886.e5. [CrossRef] [PubMed]
146. Burian, J.; Yim, G.; Hsing, M.; Axerio-Cilies, P.; Cherkasov, A.; Spiegelman, G.B.; Thompson, C.J. The mycobacterial antibiotic resistance determinant WhiB7 acts as a transcriptional activator by binding the primary sigma factor SigA (RpoV). *Nucleic Acids Res.* **2013**, *41*, 10062–10076. [CrossRef] [PubMed]
147. Varghese, S.; Tang, Y.; Imlay, J.A. Contrasting sensitivities of Escherichia coli aconitases A and B to oxidation and iron depletion. *J. Bacteriol.* **2003**, *185*, 221–230. [CrossRef]
148. Gardner, P.R.; Fridovich, I. Superoxide sensitivity of the Escherichia coli aconitase. *J. Biol. Chem.* **1991**, *266*, 19328–19333. [CrossRef]
149. Liochev, S.I.; Fridovich, I. Superoxide generated by glutathione reductase initiates a vanadate-dependent free radical chain oxidation of NADH. *Arch. Biochem. Biophys.* **1992**, *294*, 403–406. [CrossRef]
150. Flint, D.H.; Tuminello, J.F.; Emptage, M.H. The inactivation of Fe-S cluster containing hydro-lyases by superoxide. *J. Biol. Chem.* **1993**, *268*, 22369–22376. [CrossRef]
151. Kuo, C.F.; Mashino, T.; Fridovich, I. alpha, beta-Dihydroxyisovalerate dehydratase. A superoxide-sensitive enzyme. *J. Biol. Chem.* **1987**, *262*, 4724–4727. [CrossRef]
152. Ollagnier-de Choudens, S.; Loiseau, L.; Sanakis, Y.; Barras, F.; Fontecave, M. Quinolinate synthetase, an iron-sulfur enzyme in NAD biosynthesis. *FEBS Lett.* **2005**, *579*, 3737–3743. [CrossRef]
153. Flint, D.H.; Smyk-Randall, E.; Tuminello, J.F.; Draczynska-Lusiak, B.; Brown, O.R. The inactivation of dihydroxy-acid dehydratase in Escherichia coli treated with hyperbaric oxygen occurs because of the destruction of its Fe-S cluster, but the enzyme remains in the cell in a form that can be reactivated. *J. Biol. Chem.* **1993**, *268*, 25547–25552. [CrossRef]
154. Pierrel, F.; Hernandez, H.L.; Johnson, M.K.; Fontecave, M.; Atta, M. MiaB protein from Thermotoga maritima. Characterization of an extremely thermophilic tRNA-methylthiotransferase. *J. Biol. Chem.* **2003**, *278*, 29515–29524. [CrossRef] [PubMed]
155. Nicolet, Y.; Rohac, R.; Martin, L.; Fontecilla-Camps, J.C. X-ray snapshots of possible intermediates in the time course of synthesis and degradation of protein-bound Fe4S4 clusters. *Proc. Natl. Acad. Sci. USA* **2013**, *110*, 7188–7192. [CrossRef] [PubMed]
156. Outten, F.W.; Djaman, O.; Storz, G. A suf operon requirement for Fe-S cluster assembly during iron starvation in Escherichia coli. *Mol. Microbiol.* **2004**, *52*, 861–872. [CrossRef]

157. Mandin, P.; Chareyre, S.; Barras, F. A Regulatory Circuit Composed of a Transcription Factor, IscR, and a Regulatory RNA, RyhB, Controls Fe-S Cluster Delivery. *Mbio* **2016**, *7*, e00966-16. [CrossRef]
158. Esquilin-Lebron, K.; Dubrac, S.; Barras, F.; Boyd, J.M. Bacterial Approaches for Assembling Iron-Sulfur Proteins. *Mbio* **2021**, *12*, e0242521. [CrossRef]
159. Mehta, M.; Singh, A. Mycobacterium tuberculosis WhiB3 maintains redox homeostasis and survival in response to reactive oxygen and nitrogen species. *Free Radic. Biol. Med.* **2019**, *131*, 50–58. [CrossRef]
160. Py, B.; Barras, F. Building Fe-S proteins: Bacterial strategies. *Nat. Rev. Microbiol.* **2010**, *8*, 436–446. [CrossRef]
161. Roberts, C.A.; Al-Tameemi, H.M.; Mashruwala, A.A.; Rosario-Cruz, Z.; Chauhan, U.; Sause, W.E.; Torres, V.J.; Belden, W.J.; Boyd, J.M. The Suf Iron-Sulfur Cluster Biosynthetic System Is Essential in Staphylococcus aureus, and Decreased Suf Function Results in Global Metabolic Defects and Reduced Survival in Human Neutrophils. *Infect. Immun.* **2017**, *85*, e00100-17. [CrossRef]
162. Perard, J.; Ollagnier de Choudens, S. Iron-sulfur clusters biogenesis by the SUF machinery: Close to the molecular mechanism understanding. *J. Biol. Inorg. Chem.* **2018**, *23*, 581–596. [CrossRef]
163. Selbach, B.P.; Chung, A.H.; Scott, A.D.; George, S.J.; Cramer, S.P.; Dos Santos, P.C. Fe-S cluster biogenesis in Gram-positive bacteria: SufU is a zinc-dependent sulfur transfer protein. *Biochemistry* **2014**, *53*, 152–160. [CrossRef] [PubMed]
164. Albrecht, A.G.; Netz, D.J.; Miethke, M.; Pierik, A.J.; Burghaus, O.; Peuckert, F.; Lill, R.; Marahiel, M.A. SufU is an essential iron-sulfur cluster scaffold protein in Bacillus subtilis. *J. Bacteriol.* **2010**, *192*, 1643–1651. [CrossRef] [PubMed]
165. Santos, P.C.D.B. subtilis as a Model for Studying the Assembly of Fe–S Clusters in Gram-Positive Bacteria. In *Methods in Enzymolology*; Academic Press: Cambridge, MA, USA, 2017; Volume 595, p. 186.
166. D'Angelo, F.; Fernández-Fueyo, E.; Garcia, P.S.; Shomar, H.; Pelosse, M.; Manuel, R.R.; Büke, F.; Liu, S.; van den Broek, N.; Duraffourg, N.; et al. Cellular assays identify barriers impeding iron-sulfur enzyme activity in a non-native prokaryotic host. *eLIFE* **2022**, *11*, e70936. [CrossRef] [PubMed]
167. Mashruwala, A.A.; Bhatt, S.; Poudel, S.; Boyd, E.S.; Boyd, J.M. The DUF59 Containing Protein SufT Is Involved in the Maturation of Iron-Sulfur (FeS) Proteins during Conditions of High FeS Cofactor Demand in Staphylococcus aureus. *PLoS Genet.* **2016**, *12*, e1006233. [CrossRef] [PubMed]
168. Willemse, D.; Weber, B.; Masino, L.; Warren, R.M.; Adinolfi, S.; Pastore, A.; Williams, M.J. Rv1460, a SufR homologue, is a repressor of the suf operon in Mycobacterium tuberculosis. *PLoS ONE* **2018**, *13*, e0200145. [CrossRef]
169. Anand, K.; Tripathi, A.; Shukla, K.; Malhotra, N.; Jamithireddy, A.K.; Jha, R.K.; Chaudhury, S.N.; Rajmani, R.S.; Ramesh, A.; Nagaraja, V.; et al. Mycobacterium tuberculosis SufR responds to nitric oxide via its 4Fe-4S cluster and regulates Fe-S cluster biogenesis for persistence in mice. *Redox Biol.* **2021**, *46*, 102062. [CrossRef]
170. Tamuhla, T.; Joubert, L.; Willemse, D.; Williams, M.J. SufT is required for growth of Mycobacterium smegmatis under iron limiting conditions. *Microbiology* **2020**, *166*, 296–305. [CrossRef]
171. Tripathi, A.; Anand, K.; Das, M.; O'Niel, R.A.; P, S.S.; Thakur, C.; R, L.R.; Rajmani, R.S.; Chandra, N.; Laxman, S.; et al. Mycobacterium tuberculosis requires SufT for Fe-S cluster maturation, metabolism, and survival in vivo. *PLoS Pathog.* **2022**, *18*, e1010475. [CrossRef]
172. Huet, G.; Castaing, J.P.; Fournier, D.; Daffe, M.; Saves, I. Protein splicing of SufB is crucial for the functionality of the Mycobacterium tuberculosis SUF machinery. *J. Bacteriol.* **2006**, *188*, 3412–3414. [CrossRef]
173. Topilina, N.I.; Green, C.M.; Jayachandran, P.; Kelley, D.S.; Stanger, M.J.; Piazza, C.L.; Nayak, S.; Belfort, M. SufB intein of Mycobacterium tuberculosis as a sensor for oxidative and nitrosative stresses. *Proc. Natl. Acad. Sci. USA* **2015**, *112*, 10348–10353. [CrossRef]
174. Cortes, T.; Schubert, O.T.; Banaei-Esfahani, A.; Collins, B.C.; Aebersold, R.; Young, D.B. Delayed effects of transcriptional responses in Mycobacterium tuberculosis exposed to nitric oxide suggest other mechanisms involved in survival. *Sci. Rep.* **2017**, *7*, 8208. [CrossRef] [PubMed]
175. Kurthkoti, K.; Amin, H.; Marakalala, M.J.; Ghanny, S.; Subbian, S.; Sakatos, A.; Livny, J.; Fortune, S.M.; Berney, M.; Rodriguez, G.M. The Capacity of Mycobacterium tuberculosis To Survive Iron Starvation Might Enable It To Persist in Iron-Deprived Microenvironments of Human Granulomas. *Mbio* **2017**, *8*, e01092-17. [CrossRef] [PubMed]
176. Braymer, J.J.; Freibert, S.A.; Rakwalska-Bange, M.; Lill, R. Mechanistic concepts of iron-sulfur protein biogenesis in Biology. *Biochim. Biophys. Acta Mol. Cell. Res.* **2021**, *1868*, 118863. [CrossRef] [PubMed]